enough. Also, the physical dimensions of microwave circuits typically are no longer small with respect to the wavelength. A cable, connecting the port of a device under test with the measurement equipment, may easily transform the intended open circuit into a short, if its length happens to be an odd multiple of $\lambda/4$. Furthermore, short- or open-circuiting network ports, invariably linked to voltage and current measurements, may alter the behavior of microwave circuits (e.g., an amplifier, operated at those impedance extremes, may oscillate). And in waveguides, voltage and current are not even defined.

The above difficulties are circumvented if the network is embedded between defined generator and load impedances Z_0 (typically real and 50 Ω) and described in terms of its power transfer characteristics. The "scattering" of the incident power wave a_1 into the transmitted wave b_2 and the reflected wave b_1 fully characterizes the two-port network of Fig. 1 in the forward direction.

Conceptually, waves represent the propagation of energy along a transmission line. The incident (forward) wave $a = U_f/\sqrt{Z_0}$ travels along the line, with a portion of it ($b = U_r/\sqrt{Z_0}$) being reflected at the line's end. Adding both complex quantities in every location along the transmission line yields a sine-shaped pattern, the standing wave (Fig. 2). The ratio of its maximum to its minimum voltage is called the voltage standing wave ratio (VSWR) and is directly linked to the magnitude of the impedance Z_L, terminating the line.

$$\mathrm{VSWR} = \frac{|U_f| + |U_r|}{|U_f| - |U_r|} = \frac{U_{\max}}{U_{\min}} = \begin{cases} \left|\dfrac{Z_L}{Z_0}\right|, & |Z_L| > Z_0 \\ \left|\dfrac{Z_0}{Z_L}\right|, & |Z_L| < Z_0 \end{cases} \tag{1}$$

STANDING WAVE METERS AND NETWORK ANALYZERS

MEASUREMENT OF NETWORKS AT MICROWAVE FREQUENCIES

Determining the characteristics of electrical networks (network analysis) is an important measurement tool both for developers of electrical circuits and systems and in production testing. The measurement of network characteristics at microwave frequencies employs different concepts than are used at lower frequencies, where measuring port voltages and currents readily allows determination of impedance (Z) or admittance (Y) parameters. At higher frequencies, neither high-impedance voltage probes nor low-impedance current measurements are feasible, because parasitic capacitance and inductance of probes (L_s and C_p in Fig. 1) cannot be made small

The incident and reflected waves a_i and b_i at a network port (Fig. 1) are defined as linear combinations of the port currents and voltages:

$$a_i = \frac{U_i + I_i Z_0}{2\sqrt{Z_0}}, \quad b_i = \frac{U_i - I_i Z_0}{2\sqrt{Z_0}}$$

making it easy to compute the impedance Z_i at that port:

$$Z_i = \frac{U_i}{I_i} = Z_0 \frac{1 + \dfrac{b_i}{a_i}}{1 - \dfrac{b_i}{a_i}} = Z_0 \frac{1 + \Gamma_i}{1 - \Gamma_i}, \quad \Gamma_i = \frac{b_i}{a_i} \tag{2}$$

Γ is called the reflection coefficient. Similarly, the portion of the incident power transmitted from port i to port j is obtained by the transmission factor $t_{ji} = b_j/a_i$.

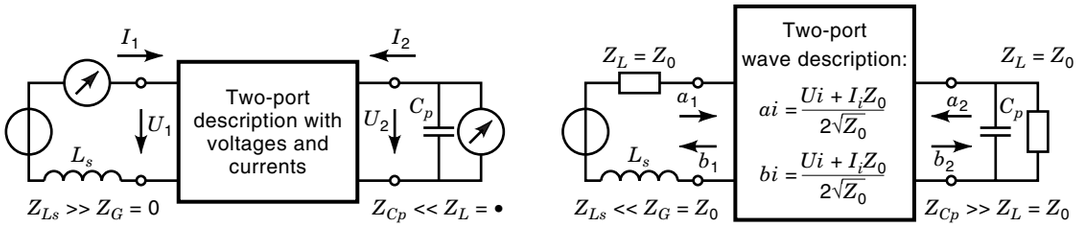

Figure 1. Drawbacks of voltage and current measurement versus the wave concept.

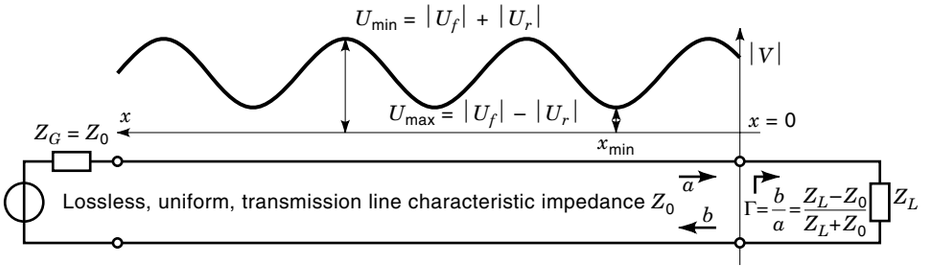

Figure 2. Standing waves along a transmission line, terminated in Z_L.

In general, a two-port network is fully characterized by its 2×2 scattering matrix,

$$\begin{pmatrix} b_1 \\ b_2 \end{pmatrix} = \begin{bmatrix} S_{11} & S_{12} \\ S_{21} & S_{22} \end{bmatrix} \begin{pmatrix} a_1 \\ a_2 \end{pmatrix}$$

which is composed of

$$\text{Reflection coefficients:} \quad S_{11} = \left.\frac{b_1}{a_1}\right|_{a_2=0}, \quad S_{22} = \left.\frac{b_2}{a_2}\right|_{a_1=0}$$

$$\text{Transmission coefficients:} \quad S_{21} = \left.\frac{b_2}{a_1}\right|_{a_2=0}, \quad S_{12} = \left.\frac{b_1}{a_2}\right|_{a_1=0}$$

The exact determination of scattering parameters, however, still requires the locus, where they are valid, to be fixed. If the measurement port at $x = 0$ in Fig. 2 is shifted to the left, the phase of incident and reflected waves changes and so does the reflection coefficient, which therefore depends on the locus. Especially at small wavelengths, measurement of S parameters stipulates the exact definition of *where* the waves are recorded, leading to the concept of *measurement* or *reference planes.* These planes are thought to perpendicularly intersect the transmission lines leading to the ports of the network, such that the phase of the waves in each plane is constant. For scattering parameter S_{ij}, the incident wave in plane j is thus the reference for the emanating wave in plane i. S_{ij} therefore describes the transmission of energy between those planes.

Since scattering parameters are ratios of emanating and incident waves, their computation does not require absolute measurement of the wave quantities. This important advantage allows the measurement of scattering parameters (with network analyzers) to inherently exhibit much higher precision than can be expected from a spectrum analyzer that relies on absolute measurement of its input power.

The remainder of this article will present a number of measurement systems for the determination of reflection coefficients (one-port network analyzer or reflectometer) and for full characterization of two-port networks. Although the concept of S-parameters is easily extended to N-ports, measurement of networks with more than two ports will not be covered, because most commercially available hardware is built for two-port measurements and can be used to characterize N-ports by simply terminating the unused N-2 ports in Z_0.

REFLECTION MEASUREMENT TECHNIQUES

The Slotted Line for VSWR and Impedance Measurements

A very old technique for measuring the VSWR on a transmission line, to determine the impedance connected at its end, makes use of a slotted transmission line of characteristic impedance Z_0 (see, for example, Ref. 1, Chap. 2, for a very detailed outline; or see Ref. 2, Chap. 4).

The slot allows a small enough probe, as not to disturb the line's field, to be moved along the x axis of the transmission line and sample its electric field. The high-frequency voltage is converted to direct current (dc) by a diode detector and brought to an instrument for readout. Since the signal level of the probe must be kept low in order to avoid loading of the line, the detector operates in its square-law region and its output is proportional to the detected *power,* or the square of the voltage. Noting the maximum and minimum values of the detector output, while varying the position of the probe, allows computation of the VSWR, provided that the slot is long enough to reach both maximum and minimum.

As indicated by Eq. (1), measurement of the scalar VSWR is not sufficient to uniquely determine the complex impedance Z_L, terminating the line. In fact, since

$$\text{VSWR} = \frac{|U_f| + |U_r|}{|U_f| - |U_r|} = \frac{1 + \left|\dfrac{U_r}{U_f}\right|}{1 - \left|\dfrac{U_r}{U_f}\right|} = \frac{1 + \left|\dfrac{b}{a}\right|}{1 - \left|\dfrac{b}{a}\right|}$$

$$= \frac{1 + |\Gamma|}{1 - |\Gamma|} \rightarrow |\Gamma| = \frac{\text{VSWR} - 1}{\text{VSWR} + 1}$$

only the *magnitude* of the reflection coefficient Γ is available. The *phase* of Γ is obtained by noting the *position* x_{min} of the first minimum, appearing when the probe is moved away from Z_L. With the propagation constant

$$\beta = \frac{2\pi}{\lambda_{sl}}$$

of the slotted transmission line, the phase of Γ becomes

$$\varphi = 2\beta x - \pi$$

such that

$$\Gamma = |\Gamma| e^{j\varphi} = \frac{\text{VSWR} - 1}{\text{VSWR} + 1} e^{j(2\beta x - \pi)}$$

and the complex impedance Z_L may be computed from Γ using Eq. (2).

Though conceptionally simple, the slotted line technique suffers from a number of drawbacks and limitations:

1. The slotted transmission line itself is a costly precision device, exhibiting precise line impedance Z_0, low losses,

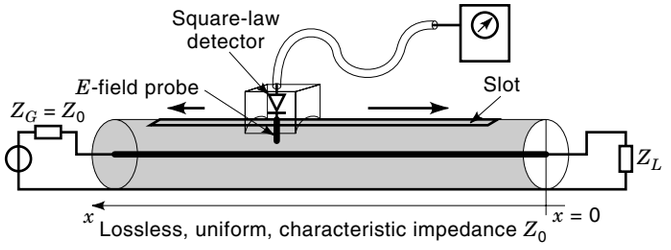

Figure 3. The slotted line measurement setup.

negligible loading due to the probe, and mechanical stability of the probe depth over the entire moving range.

2. Linearity errors and the limited dynamic range of the detectors reduce the accuracy when measuring large VSWRs. By modulating the RF source and selective reception of the modulation frequency, noise can be reduced, increasing sensitivity and thus measurement dynamic (the so-called "modulated frequency technique").
3. The measurement procedure requires manual interaction and, in its simple form of Fig. 3, does not allow for swept frequency impedance measurements. If, however, only the magnitude of the reflection coefficient is of interest, Sorger (3) describes a setup that uses two slotted lines for swept frequency VSWR measurement.

Because slotted line reflection measurements are a very old technique, much research has been undertaken to alleviate the above limitations. Many ideas and extensions can be found in Ref. 2, covering the topic in more detail.

Using the Slotline with Multiple Probes

The biggest drawback of slotline measurements, the need for manual interaction, can be overcome if more than one probe taps to the field of the line in known and fixed positions. Figure 4 shows a system proposed by Caldecott (4) that uses three probes in arbitrary but known positions x_1, x_2, and x_3. Caldecott proved that

$$\Gamma_L \approx \frac{P_1(e^{-j2\beta x_2} - e^{-j2\beta x_3}) + P_2(e^{-j2\beta x_3} - e^{-j2\beta x_1}) + P_3(e^{-j2\beta x_1} - e^{-j2\beta x_2})}{\sin[2\beta(x_2 - x_3)]\sin[2\beta(x_3 - x_1)] + \sin[2\beta(x_1 - x_2)]}$$

even providing complex measurability of the reflection coefficient, although only scalar power measurements ($P_1 \ldots P_3$) are used.

Another interesting multiprobe reflectometer for swept frequency/swept power applications reported in Ref. 5 even provided an automatic Smith-chart display of the measured impedance.

The Six-Port Reflectometer

The idea of the foregoing section can be generalized to the so-called six-port reflectometer, developed by Hoer (6) and Engen (7) in the early 1970s. Figure 5 shows a general six-port junction, driven by a signal generator at port 5, ports 1 through 4 connected to power sensors (diode detectors, bolometers, thermocouple, etc.) and port 6 interfacing to the unknown impedance with reflection coefficient Γ_L.

As the mathematical derivation of the six-port theory is rather lengthy, the interested reader should refer to Refs. 2, 6, or 7 for details. In essence the 6×6 S-matrix of the six-port network is reduced to the form

$$b_i = Q_i a_6 + R_i b_6, \quad i = 1, \ldots, 4 \tag{3}$$

by using $\Gamma_i = a_i/b_i$ to eliminate $a_1 \ldots a_5$ (b_5 is also eliminated by omitting the 5th equation). The powers P_i are related to b_i by

$$P_i = |b_i|^2(1 - |\Gamma_i|^2)$$

and, using Eq. (3), can be expressed as

$$P_i = (1 - |\Gamma_i|^2)\{|R_i|^2|b_6|^2 + 2\mathrm{Re}(Q_i^* R_i)\mathrm{Re}(a_6 b_6^*) + 2\mathrm{Im}(Q_i^* R_i)\mathrm{Im}(a_6 b_6^*) + |Q_i|^2|a_6|^2\}$$

which may be written in matrix form as

$$(P_1 P_2 P_3 P_4)^T = [D](|b_6|^2\ \mathrm{Re}(a_6 b_6^*)\ \mathrm{Im}(a_6 b_6^*)\ |a_6|^2)^T \tag{4}$$

with $[D]$ being a real-valued 4×4 matrix. Inverting Eq. (4) gives access to its right-hand-side vector, provided that $[D]$ is known and invertible with $[C]$ being its inverse,

$$(|b_6|^2\ \mathrm{Re}(a_6 b_6^*)\ \mathrm{Im}(a_6 b_6^*)\ |a_6|^2)^T = [C](P_1 P_2 P_3 P_4)^T$$

such that Γ_L can be computed as

$$\Gamma_L = \frac{a_6}{b_6} = \frac{a_6 b_6^*}{b_6 b_6^*} = \frac{\mathrm{Re}(a_6 b_6^*) + j\,\mathrm{Im}(a_6 b_6^*)}{|b_6|^2} = \frac{\sum_{n=1}^{4} C_{2n} P_n + j \sum_{n=1}^{4} C_{3n} P_n}{\sum_{n=1}^{4} C_{1n} P_n} \tag{5}$$

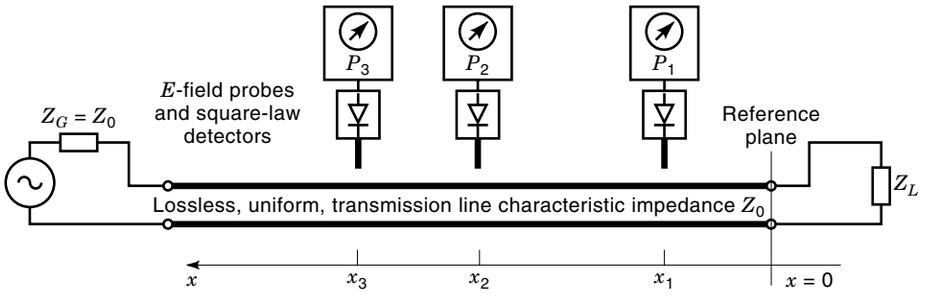

Figure 4. The multiprobe reflectometer.

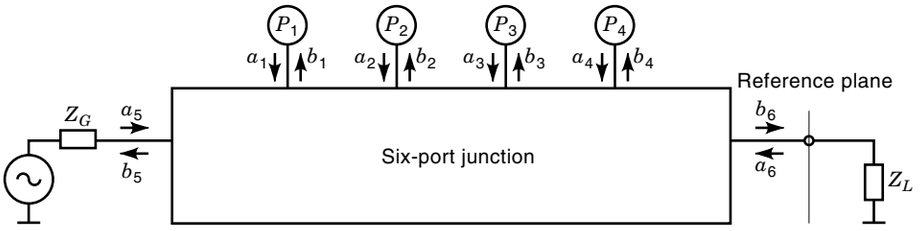

Figure 5. The six-port reflectometer.

With just 12 of the 16 real-valued elements of [C] appearing in Eq. (5), only 11 need to be computed, as Eq. (5) may be normalized to one of the 12 terms. They are determined by measuring *six known* reflection coefficients and using the complex equation [Eq. (5)] to establish a set of 12 linear, real-valued equations in the 12 unknowns.

Although such a calibration procedure to determine the elements of [C] *must* be carried out before the six-port can be used for reflection measurements, it has the added advantage of providing error-corrected results. No a priori knowledge about the six-port is necessary, because the calibration sufficiently characterizes [C], which reflects the properties of the six-port junction.

Further advantages of this kind of instrument are that neither the signal generator nor the power sensors need to be perfectly matched. The mismatch of the power sensors must however be constant. Because only ratios of measured powers enter the calculation of Γ_L, the power sensors do not need to be absolutely calibrated for power measurements.

However, the power sensors must be linear; and because of their broadband nature, care must be taken to suppress spurious emissions from the signal generator.

Evaluation of Eq. (5) and the determination of [C] require some amount of numerical processing. Six-port reflectometers are therefore almost always combined with microcontrollers to automate the process of calibration and measurement.

Internally, the six-port must be built such that the reduced matrix [D] is invertible at all measurement frequencies. Details of the design process are outlined in Ref. 8 with a practical realization, using 0° and 90° couplers described in Ref. 9.

Reflection Measurement with the Directional Coupler

All of the impedance measurement methods described thus far evaluate the *sum* of incident and reflected waves, requiring at least two independent measurements for calculation of the reflection coefficient.

Alternatively, forward and reflected waves may be separated using a directional coupler. Such devices are common building blocks in microwave engineering and exist in a wide variety of designs, many of which are treated in Ref. 10, Chap. 8. The interested reader may also refer to Ref. 11 for some less common coupler structures and unusual applications. Figure 6 depicts the associated symbol of a directional coupler and its scattering matrix.

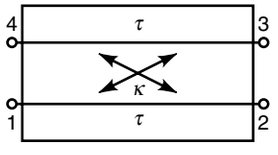

$$S_C = \begin{pmatrix} 0 & \tau & \kappa & 0 \\ \tau & 0 & 0 & \kappa \\ \kappa & 0 & 0 & \tau \\ 0 & \kappa & \tau & 0 \end{pmatrix}$$

Figure 6. The directional coupler.

The important property of the directional coupler, used to separate incident and reflected wave is in its decoupled port. Figure 7 illustrates that feeding a wave a_1 into port 1 results in wave $b_2 = \tau a_1$ and $b_3 = \kappa a_1$ being emitted at ports 2 and 3 with no energy being fed to port 4, the decoupled port. Similarly, port 2 is decoupled from port 3. Driving the coupler at port 1, terminating port 3 in Z_0, and connecting a matched power detector to port 4 allows measurement of unknown reflection coefficients connected to port 2.

Directional couplers, also called "VSWR-bridges" or "reflection coefficient bridges," appear in various forms, with the microstrip coupler, the resistive coupler, and the Wilkinson divider (Fig. 8) being the variants most often found.

All practical realizations of directional couplers exhibit finite *directivity,* meaning that a small amount of the power fed to port 1 will leak to port 4, even if port 2 and 3 are perfectly terminated in Z_0. The directivity of a coupler is defined as

$$d = \frac{S_{14}}{\kappa\tau}$$

Mismatch at port 2 and even at the driving port 1 will further add to erroneous reflections being indicated by the wave b_4, which ideally should be a measure of the reflection of Z_L only. All these errors must be kept low if the coupler is to be used for precision reflection measurement. Narrow-band precision couplers, exhibiting more than 50 dB directivity, have been built in waveguide and broad-band couplers, typically of the resistive bridge type, and exhibit more than 36 dB directivity over a bandwidth of more than three decades. As a rule of thumb, the directivity should be at least 10 dB better than the expected reflection coefficient of the measured device under test (DUT).

ARCHITECTURES OF NETWORK ANALYZERS

In order to measure the entire scattering matrix of a two-port, some means of measuring the transmitted waves as well as

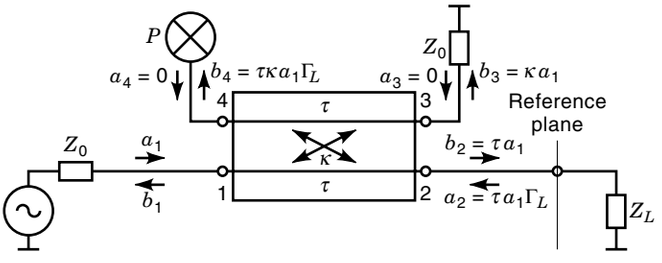

Figure 7. Reflection measurement using a directional coupler.

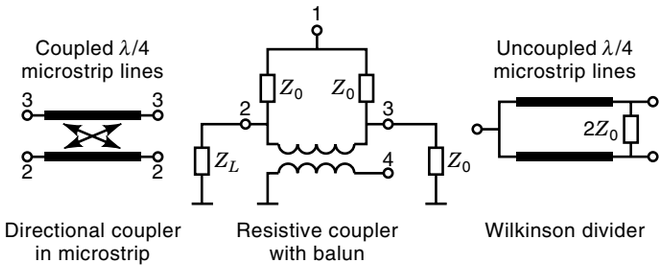

Figure 8. Some commonly used directional couplers.

the reflected waves must be provided. Because reflection measurements, nowadays, are almost always carried out with directional couplers, we will use its symbol for denoting measurement of reflected waves. As in Fig. 7, the "mixer" symbol will be used to denote a measurement point, at which the wave to be measured may be further processed in one of the following ways:

1. With power detectors, leading to scalar measurement of the wave
2. With a homodyne receiver, potentially capable of providing amplitude and phase information
3. With a heterodyne receiver (hence the mixer symbol), providing amplitude and phase information

Depending on the type of detector used, network analyzers (NAs) are classified into one of the following types of analyzer:

Scalar Network Analyzer. The simplest and most economic approach to the measurement of scattering-parameters employs power (diode) detectors. Because these provide no phase information, only the magnitude of the S-parameters can be measured, hence the term *scalar network analyzer* (SNA). For many applications, however, the magnitude may be all that is needed. Calibration techniques, as described in the section entitled "Error Models, Calibration, and Error Correction," however, require the phase information and consequently cannot be applied to SNAs. Instead, normalization is all that can be employed with such an instrument.

Other drawbacks of SNAs are the limited dynamic range and the broad-band nature of the power detectors. Since they record the entire power of a wave, regardless of its spectral origin, these instruments are susceptible to spurs or harmonics of the generator. If, for example, the harmonics of the radio-frequency (RF) source are suppressed by 30 dB, and the DUT has high-pass or band-stop characteristic (return loss of a filter or an antenna), the SNA will show no less than −30 dB attenuation or return loss, regardless of the DUT's real properties.

It should be emphasized that the mere use of power detectors does not necessarily yield a scalar network analyzer. The six-port reflectometer, as described in the section entitled "The Six-Port Reflectometer," employs four scalar detectors to determine the complex reflection coefficient; a complete vector NA can be built by using two such reflectometers (see Refs. 8, 9, and 12), retaining all vector error-correction capabilities of those instruments (13,14), as discussed in the section entitled "Error Models, Calibration, and Error Correction."

Heterodyne (Vector) Network Analyzer. If the wave quantities are processed by heterodyne receivers, the phase information can be preserved by phase-locking the heterodyne oscillator to the RF source driving the DUT (Fig. 9), and complex measurement of the scattering parameters is possible. Besides providing a much higher dynamic range (over 120 dB for recent industry products versus 70 dB for SNAs), the ability to measure the complex S-parameters has the added benefit of allowing calibration techniques to enhance measurement accuracy. On the other hand, the inherent higher complexity of heterodyne vector network analyzers (VNAs) results in more expensive hardware. For broad-band systems, the heterodyne oscillator and its Phase Locked Loop (PLL) add considerably to the cost, because they must cover the system's entire bandwidth.

A cost reducing alternative exists by employing "harmonic mixing" (e.g., Ref. 35). In this case the local oscillator (LO) in Fig. 9 has to cover only one octave with all higher frequencies that are needed being supplied by the LO's harmonics. Harmonic mixing, however, leads to higher mixer conversion loss and thus also reduces the instrument's dynamic range.

Homodyne Network Analyzers. In order to circumvent the need for a second microwave source and phase-locking circuitry, homodyne systems use the same generator for down-conversion that drives the DUT. Because the homodyne mixing process provides only the real part of the wave quantity, homodyne NAs need additional hardware (phase-shifters) to extract the complex information from two or more measurements (e.g., Ref. 15). Though relatively simple hardware concepts have been developed (16), homodyne NAs also suffer from their sensitivity to generator harmonics, limiting dynamic range. It is for that reason that homodyne systems are rarely used in the laboratory, although some realizations exist for industrial measurements.

Regardless of the kind of detector used, all practical realizations of the NA architectures introduced in the next sections should be built to provide

- Good port match, properly terminating the DUT in the system impedance Z_0
- High directivity of the directional coupler for precise reflection measurement
- Low variation of transmission losses over the bandwidth of the system

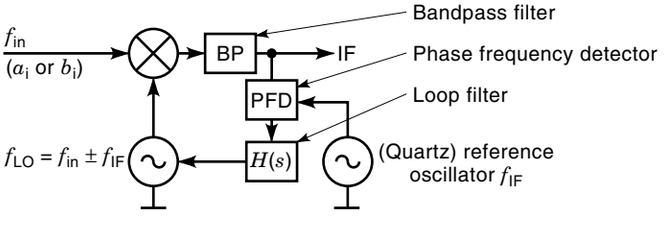

Figure 9. Heterodyne receiver (LO): Local Oscillator, IF: Intermediate Frequency, BP: Bandpass filter, PFD: Phase-Frequency Detector, $H(s)$: Loopfilter.

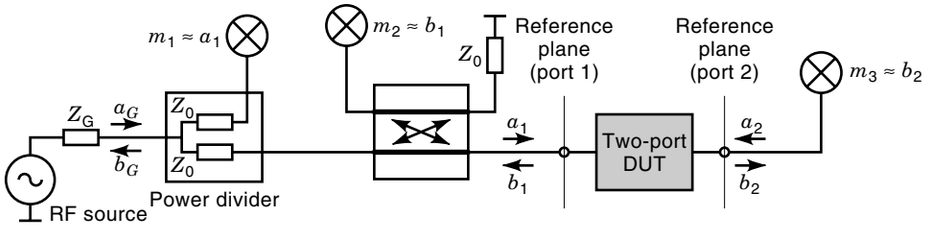

Figure 10. Unidirectional network analyzer.

Reflection and Transmission Measurement with the Unidirectional Network Analyzer

Unidirectional network analyzers (Fig. 10) extend the capability of a simple reflectometer to measure S_{11} and S_{21} of a two-port DUT.

With the measured quantity m_1 being proportional to a_1, m_2 presenting a measure for the reflection b_1, and m_3 presenting a measure for the transmission b_2, S_{11}, and S_{21} can be expressed as

$$S_{11} = c_{11}\frac{m_2}{m_1}, \quad S_{21} = c_{21}\frac{m_3}{m_1} \tag{6}$$

The proportionality constants are usually obtained through normalization measurements of known reflection/transmission coefficients. Connecting a "Short" with $S_{11} = -1$ to port 1 yields

$$c_{11} = -1\frac{m_1^S}{m_2^S}; \quad \text{and} \quad c_{21} = 1\frac{m_1^T}{m_3^T}$$

is obtained by connecting both ports ("Through"), such that $S_{21} = 1$.

For measurement of S_{22} and S_{12} (reverse direction), the DUT must be connected to the unidirectional NA with its ports reversed.

The Three-Receiver Network Analyzer Architecture for Full Two-Port Measurements

The need for manually reversing the DUT can be eliminated if a switch and another directional coupler is introduced into the system of Fig. 11. With the switch in position I, the RF source is connected to port 1 of the DUT, m_1 is proportional to a_1, m_2 is a measure for b_1, and m_3 is a measure for b_2. The second contact of the switch terminates the coupler at port 2 in Z_0, ensuring proper port match. With the switch in position II, port 2 of the DUT is excited, the coupler connected to port 1 of the DUT is terminated in Z_0, and m_1 is now a measure for a_2. Since the three receivers m_1, m_2, and m_3 now provide different readings, depending upon the position of the switch, their measurement values will from now on be referred to as m_i^{I} and m_i^{II}, the superscript denoting the position of the switch. The S-parameters of the DUT are therefore determined as

$$S_{11} = c_{11}\frac{m_2^{\mathrm{I}}}{m_1^{\mathrm{I}}}, \quad S_{21} = c_{21}\frac{m_3^{\mathrm{I}}}{m_1^{\mathrm{I}}}$$

$$S_{22} = c_{22}\frac{m_3^{\mathrm{II}}}{m_1^{\mathrm{II}}}, \quad \text{and} \quad S_{12} = c_{12}\frac{m_2^{\mathrm{II}}}{m_1^{\mathrm{II}}}$$

with the proportionality constants resulting from normalization measurements. Using a "Short" at port 1 and port 2 and a "Through" connecting both ports yields

$$c_{11} = -1\frac{m_1^{\mathrm{I}}}{m_2^{\mathrm{I}}}, \quad c_{21} = 1\frac{m_1^{\mathrm{I}}}{m_3^{\mathrm{I}}}$$

$$c_{22} = -1\frac{m_1^{\mathrm{II}}}{m_3^{\mathrm{II}}}, \quad \text{and} \quad c_{12} = 1\frac{m_1^{\mathrm{II}}}{m_2^{\mathrm{II}}}$$

The switch should be well-matched to keep measurement errors low, must be reproducible, and must provide sufficient isolation in order not to limit the dynamic range of the instrument.

The Four-Receiver Vector Network Analyzer

There seems to be little gained in extending the above-described three-receiver NA with a fourth receiver, as outlined in Fig. 12, since the complete S-matrix of a two-port can already be measured with three receivers. For *vector* network

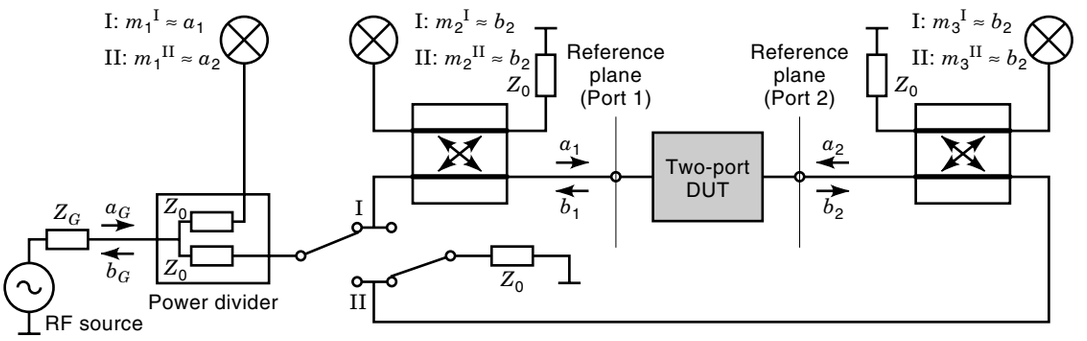

Figure 11. Bidirectional network analyzer with three receivers.

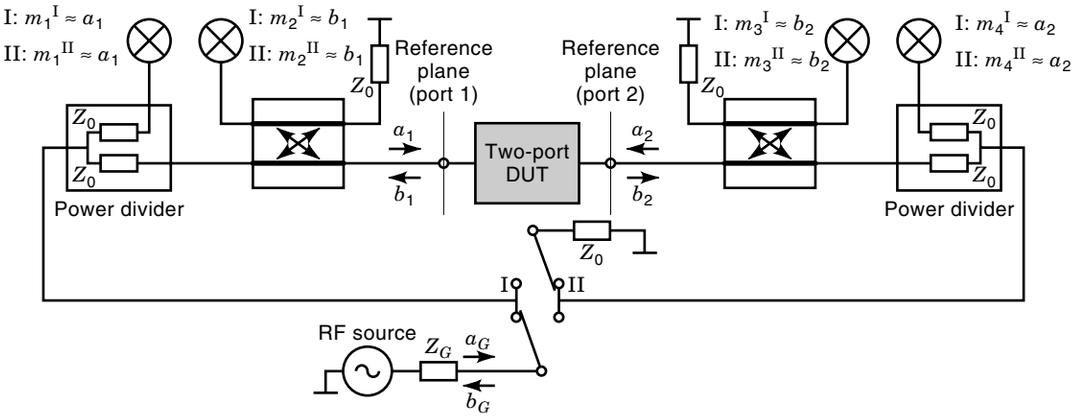

Figure 12. Bidirectional vector network analyzer with four receivers.

analyzers (VNA), however, the additional receiver provides simultaneous measurement capability of all waves and makes the architecture completely symmetrical around the DUT, resulting in interesting calibration capabilities, detailed in the sections entitled "The Seven-Term Error Model for Vector Network Analyzers with Four Receivers," "The Cross-Talk Correcting 15-Term Error Model for Four-Receiver VNAs," and "Modern Self-Calibration Techniques for Four-Receiver VNAs." The subtle change of moving the switch from *between* two receivers to *in front* of the receiver pairs radically alters the error model, even reducing the requirements of the switch (see section entitled "The Seven-Term Error Model for Vector Network Analyzers with Four Receivers"). For measurements *without* error correction, however, the switch must, again, be as ideal as possible with respect to match, repeatability, and isolation.

A four-receiver VNA measures the S-matrix of a two-port DUT as

$$S_{11} = c_{11}\frac{m_2^{\mathrm{I}}}{m_1^{\mathrm{I}}}, \quad S_{21} = c_{21}\frac{m_3^{\mathrm{I}}}{m_1^{\mathrm{I}}}$$
$$S_{22} = c_{22}\frac{m_3^{\mathrm{II}}}{m_4^{\mathrm{II}}}, \quad \text{and} \quad S_{12} = c_{12}\frac{m_2^{\mathrm{II}}}{m_4^{\mathrm{II}}}$$

with the proportionality factors determined through normalization measurements as described before.

ERROR MODELS, CALIBRATION, AND ERROR CORRECTION

For a long time, precision NAs required carefully designed and expensive hardware, ensuring a good port match for embedding the DUT between proper terminations and high coupler directivity for precise reflection measurement. Losses in the hardware had to be accounted for by reference measurements of devices with known characteristic. With the advent of microprocessors, however, the focus has shifted toward calibration techniques that allow the imperfections of the hardware to be taken into account and corrected mathematically. An error model is needed for this purpose, and its parameters are determined through measurement of well-known one- or two-ports (calibration). This mathematical description of the nonideal hardware is then used to correct the measurement of the DUT.

The error models, covered in subsequent sections, are used to model and correct all the linear errors of the VNA: transmission losses between the generator, the receivers, and the DUT; port match; and coupler directivity. Theoretically, the hardware of a VNA that provides these error-correction capabilities need no longer be built to high standards. Yet, commercially available systems still strive for good hardware performance for two reasons: first, in an effort to assist the calibration through good hardware performance and achieve even better accuracy; and, second, to provide an instrument that does not depend upon time consuming calibration procedures, allowing uncorrected measurements for all those applications that can tolerate the reduced accuracy. However, there are commercially available instruments that use the calibration capabilities for a considerable extension of their usable bandwidth. When the directivity of the directional couplers decreases to unsatisfactory values below a certain frequency, a built-in error correction mathematically enhances the directivity to usable values, extending the frequency range to as low as 9 kHz.

Since all error models presented herein are linear and deterministic, there remains a stringent requirement that the VNA hardware be linear (errors due to compression of receivers cannot be corrected) and stable.

With modern equipment achieving a short-term stability in the millidecibel range, the most prominent source of error in many cases remains in the cabling between the VNA and the DUT and the associated interface contacts. These contacting errors are statistical in nature and must be minimized by proper cable and connector selection and maintenance. As the transmission phase of coaxial cables varies over temperature and may change if the cable is bent, VNAs are usually equipped with special test-port cables, optimized for phase-stability and mechanically protected against overbending.

The mathematical descriptions of the error models presented in the following sections make heavy use of matricial representations, leading to very compact expressions and similar structures for the different models. Alternatively, flowgraph techniques could be applied as in Refs. 17 and 18, leading to comparable results.

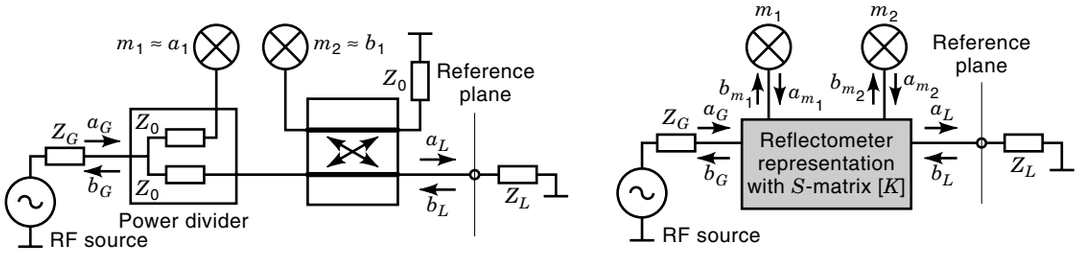

Figure 13. Four-port description of a reflectometer.

The Three-Term Error Model for Reflection Measurements

A reflectometer like the one of Fig. 13 can always be represented by a linear four-port, driven at the left port by the RF source, two ports connected to the receivers for measurement of the incident and reflected waves and the DUT placed at the port to the right. In this general form, the underlying hardware of the reflectometer becomes unimportant, much like the fact that internal structure of the six-port reflectometer was of no concern in the section entitled "The Six-Port Reflectometer."

The waves incident to and reflected from this four-port relate to its S-matrix by

$$\begin{pmatrix} b_{m_1} \\ b_{m_2} \\ a_L \\ b_G \end{pmatrix} = [K] \begin{pmatrix} a_{m_1} \\ a_{m_2} \\ b_L \\ a_G \end{pmatrix} \tag{7}$$

The measured quantities m_1 and m_2 are proportional to the incident waves of the receivers ($m_1 = \eta_1 b_{m_1}$, $m_2 = \eta_2 b_{m_2}$), with the receiver constant η_i representing the entire transfer characteristics of the ith receiver, comprising mixer conversion, intermediate frequency (IF) amplification, and so on. Architectural details of the receiver are of no concern at this point. The only requirement is that η_i must be constant, implying stability of the receivers phase and amplitude response. Let r_i be the reflection coefficients of the receiver inputs such that the conditions

$$m_1 = \eta_1 b_{m_1}, \quad m_2 = \eta_2 b_{m_2}, \quad a_{m_1} = r_1 b_{m_1}, \quad a_{m2} = r_2 b_{m_2} \tag{8}$$

result. Their use allows the elimination of the generator waves a_G and b_G in Eq. (7), according to the following scheme: The third equation of Eq. (7) is solved for a_G and the result is inserted into the first two equations. In these, b_{m_i} is expressed through a_{m_i} and a_{m_i} in turn expressed by m_i, using Eq. (8). The resulting two equations relate the measured quantities m_1 and m_2 to the waves at the DUT and are arranged in matrix form as

$$\begin{pmatrix} b_L \\ a_L \end{pmatrix} = \begin{bmatrix} G_{11} & G_{12} \\ G_{21} & G_{22} \end{bmatrix} \begin{pmatrix} m_2 \\ m_1 \end{pmatrix} = [G] \begin{pmatrix} m_2 \\ m_1 \end{pmatrix} \tag{9}$$

Every element of $[G]$ evolves as a function of K_i, r_i, and η_i, which need not be explicitly known. It suffices to determine $[G]$ through a process called calibration, in order to calculate the correct waves at the DUT from the raw measurements m_i:

$$\Gamma_L = \frac{b_L}{a_L} = \frac{G_{11} m_2 + G_{12} m_1}{G_{21} m_2 + G_{22} m_1} \tag{10}$$

Interestingly, this four-port/two-port reduction with its elimination of the generator waves has freed the error model [Eq. (9)] from any influence of the RF source. Power or impedance variations do not introduce measurement errors, provided that m_1 and m_2 are measured simultaneously.

Equation (10) can be further simplified by dividing numerator and denominator by m_1 and defining

$$m_{11} = \frac{m_2}{m_1} = \frac{\eta_2 b_{m_2}}{\eta_1 b_{m_1}} \tag{11}$$

as the uncorrected (raw) reflection measurement [compare with Eq. (6)] such that the error-corrected reflection coefficient becomes

$$\Gamma_L = \frac{b_L}{a_L} = \frac{G_{11} m_{11} + G_{12}}{G_{21} m_{11} + G_{22}} \tag{12}$$

The importance of Eq. (11) is twofold:

1. The ratio of two measurements enters the computation of the error-corrected result. Relative, rather than absolute, measurements are therefore still sufficient if an error model and error correction is used. And with the reflected wave measurement m_2 being referenced to the incident wave measurement m_1, the theoretically derived insensitivity of the error model to power variations of the RF source becomes obvious.
2. The ratio of η_1/η_2 appearing in Eq. (11) indicates that amplitude and phase drifts of the receivers cancel if both receivers are built *equal*.

Both properties are essential for the high accuracy achievable with VNAs. The use of the latter property is especially important for accurate phase measurements at high frequencies.

Calibration of the Three-Term Error Model. Before error-corrected measurements using Eq. (12) can be carried out, the error matrix $[G]$ must be determined. For this calibration procedure, a number of one-ports (calibration standards) with known reflection coefficients are needed. Since numerator and denominator of Eq. (12) may be multiplied by any complex number without altering the result, one of the error terms

may arbitrarily be set to 1, with the other three remaining to be computed. Without loss of generality, let $G_{11} = 1$ and Eq. (12) can be rearranged to yield a linear equation in the three remaining error terms:

$$-G_{12} + \Gamma^i m_{11}^i G_{21} + \Gamma^i G_{22} = m_{11}^i \tag{13}$$

The superscript i denotes the ith calibration measurement with known reflection coefficient Γ^i and the corresponding measured value m_{11}^i. Performing calibration measurements with three distinct and known reflection standards yields three linear inhomogeneous and independent forms of Eq. (13), sufficient to solve for the needed error terms.

In order to maximize the independence of the three equations, the three-term calibration is typically performed with those three impedances, which are furthest apart in the reflection plane:

$$\text{Open:} \quad \Gamma^O = 1, \quad \text{Short:} \quad \Gamma^S = -1, \quad \text{Match:} \quad \Gamma^M = 0$$

Three-term reflectometer calibration is therefore also referred to as OSM calibration.

The Five-Term Error Model for Unidirectional Vector Network Analyzers

Extending a single reflectometer with a third receiver for transmission measurements yields the unidirectional NA of Fig. 10. Its error model comprises two parts: The reflectometer hardware to the left of the DUT which is again represented by an error two-port [G], and the hardware to the right of the DUT which constitutes a physical two-port with a corresponding 2×2 S-matrix (Fig. 14).

As in the foregoing section, the reflection coefficient r_3 and the transfer characteristics η_3 of the receiver m_3 establish the conditions

$$a_{m_3} = r_3 b_{m_3} \quad \text{and} \quad m_3 = \eta_3 b_{m_3}$$

which are used to reduce [T] to an error two-port that relates the waves a_2 and b_2 of the DUT to the measured value m_3:

$$\begin{pmatrix} b_2 \\ a_2 \end{pmatrix} = \begin{bmatrix} H_{11} & H_{12} \\ H_{21} & H_{22} \end{bmatrix} \begin{pmatrix} m_3 \\ 0 \end{pmatrix} = [H] \begin{pmatrix} m_3 \\ 0 \end{pmatrix}$$

Together with the error two-port of the reflectometer

$$\begin{pmatrix} b_1 \\ a_1 \end{pmatrix} = \begin{bmatrix} G_{11} & G_{12} \\ G_{21} & G_{22} \end{bmatrix} \begin{pmatrix} m_2 \\ m_1 \end{pmatrix} = [G] \begin{pmatrix} m_2 \\ m_1 \end{pmatrix}$$

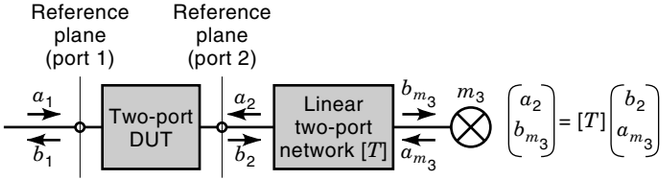

Figure 14. Hardware description of the transmission receiver m_3.

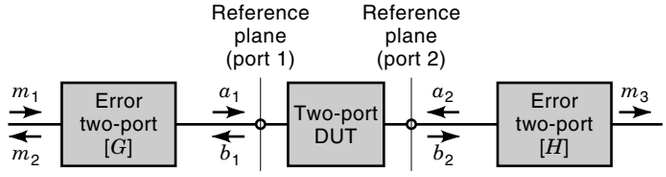

Figure 15. Error model of the unidirectional vector network analyzer.

and the definition of the DUT's S-matrix

$$\begin{pmatrix} b_1 \\ b_2 \end{pmatrix} = \begin{bmatrix} S_{11} & S_{12} \\ S_{21} & S_{22} \end{bmatrix} \begin{pmatrix} a_1 \\ a_2 \end{pmatrix} \tag{14}$$

the error model (Fig. 15) can be expressed as

$$\begin{pmatrix} b_1 \\ b_2 \end{pmatrix} = \begin{pmatrix} G_{11}m_2 + G_{12}m_1 \\ H_{11}m_3 \end{pmatrix} = [S] \begin{pmatrix} G_{21}m_2 + G_{22}m_1 \\ H_{21}m_3 \end{pmatrix} = [S] \begin{pmatrix} a_1 \\ a_2 \end{pmatrix} \tag{15}$$

It is obvious that the two equations of Eq. (15) are not sufficient to solve for the entire S-matrix of the DUT. On the other hand, the "forward" S-parameters S_{11} and S_{21} cannot be error-corrected by themselves without the knowledge of S_{12} and S_{22}.

Error correction is therefore only possible if a second measurement with the DUT reversed is made. Denoting the measured values with superscripts f and r for forward and reverse measurement of the DUT, both vector equations of Eq. (15) can be combined into a matrix equation

$$\begin{bmatrix} G_{11}m_2^f + G_{12}m_1^f & H_{11}m_3^r \\ H_{11}m_3^f & G_{11}m_2^r + G_{12}m_1^r \end{bmatrix} = [S] \begin{bmatrix} G_{21}m_2^f + G_{22}m_1^f & H_{21}m_3^r \\ H_{21}m_3^f & G_{21}m_2^r + G_{22}m_1^r \end{bmatrix} \tag{16}$$

Again, Eq. (16) may be normalized to the incident waves m_1^f and m_1^r such that only the uncorrected measurement ratios

$$m_{11} = \frac{m_2^f}{m_1^f} = \frac{\eta_2 b_{m_2}^f}{\eta_1 b_{m_1}^f}, \quad m_{21} = \frac{m_3^f}{m_1^f} = \frac{\eta_3 b_{m_3}^f}{\eta_1 b_{m_1}^f}$$

$$m_{12} = \frac{m_3^r}{m_1^r} = \frac{\eta_3 b_{m_3}^r}{\eta_1 b_{m_1}^r}, \quad m_{22} = \frac{m_2^r}{m_1^r} = \frac{\eta_2 b_{m_2}^r}{\eta_1 b_{m_1}^r}$$

remain [compare with Eq. (6)]. Solving the normalized version of Eq. (16) for [S] yields the error-correction formula

$$[S] = \begin{bmatrix} G_{11}m_{11} + G_{12} & H_{11}m_{12} \\ H_{11}m_{21} & G_{11}m_{22} + G_{12} \end{bmatrix} \times \begin{bmatrix} G_{21}m_{11} + G_{22} & H_{21}m_{12} \\ H_{21}m_{21} & H_{21}m_{22} + G_{22} \end{bmatrix}^{-1} \tag{17}$$

Calibration of the Five-Term Error Model. Not all of the eight error terms contained in [G] and [H] are needed for error correction with Eq. (17), where H_{12} and H_{22} do not appear. Fur-

thermore, the structure of Eq. (17) reveals its invariance to multiplication of *all* error terms with a constant. The remaining error terms may therefore be computed by rearranging Eq. (17) into a linear, homogeneous system of equations in the error terms,

$$\begin{bmatrix} -m_{11}^i & -1 & S_{11}^i m_{11}^i & S_{11}^i & 0 & S_{12}^i m_{21}^i \\ 0 & 0 & S_{21}^i m_{11}^i & S_{21}^i & -m_{21}^i & S_{22}^i m_{21}^i \\ 0 & 0 & S_{12}^i m_{22}^i & S_{12}^i & -m_{12}^i & S_{11}^i m_{12}^i \\ -m_{22}^i & -1 & S_{22}^i m_{22}^i & S_{22}^i & 0 & S_{21}^i m_{12}^i \end{bmatrix} \begin{pmatrix} G_{11} \\ G_{12} \\ G_{21} \\ G_{22} \\ H_{11} \\ H_{21} \end{pmatrix} = 0 \tag{18}$$

setting one error term to unity and solving the resulting inhomogeneous system of equations. $[S^i]$ denotes the S-matrix of the ith calibration standard. Five independent equations are needed to solve for the remaining five independent error terms, hence the name five-term error model.

The problem of *how many* two-port standards are needed and how they must be built to ensure five independent equations can be tackled in the following way: A suitable combination of standards must always comprise at least one standard with transmission ($S_{21} \neq 0$ and $S_{12} \neq 0$); otherwise, H_{11} and H_{21} cannot be determined [$S_{21} = S_{12} = 0$ implies $m_{21} = m_{12} = 0$, such that the fifth and sixth column of Eq. (18) vanish]. Numerical investigations reveal that a two-port standard exhibiting transmission contributes at least two equations and may contribute four if it is not symmetric (i.e., $S_{11} \neq S_{22}$).

Because the use of reflection standards ($S_{21} = S_{12} = 0$) implies $m_{21} = m_{12} = 0$, the second and third equation of Eq. (18) degenerate, leaving only the first and fourth equation for determination of $[G]$; and with $S_{11} = \Gamma_S$ the first equation corresponds directly to Eq. (13) (three-term calibration) with $G_{11} = 1$. Transmissionless standards therefore contribute one equation per reflection coefficient connected to port 1.

Even though the general nature of Eq. (18) allows for calibration with any set of standards that yields five independent equations, traditionally the five-term model is calibrated using the three reflection standards Open, Short, and Match (contributing three equations), together with a direct connection of both reference planes, the Through standard (furnishing the remaining two equations). Figure 16 depicts this commonly used set of standards. Another name for this commonly used procedure is SOLT, which stands for Short, Open, Load, and Through.

Of course, care must be taken as to build the calibration standards such that their S-matrix or reflection coefficients match the postulated values used in the calibration process. All deviations of the standards' *real* values from the postulated *ideal* of Fig. 16 lead to inconsistencies in the equations of Eq. (18). Keeping these inconsistency errors small requires a smart choice and precisely built or modeled standards.

Because the Through standard requires a direct connection of both measurement ports, it is typically a very easy standard to realize in coaxial media. The same holds for the Short, which is easily manufactured to high precision (<1° deviation at 20 GHz) in coaxial media. However, care must be taken as to ensure that the Short is connected directly to the reference plane, which is a potential problem if sexed connectors (N, SMA, K) are used. Bridging same-sexed connectors with adapters introduces a phase shift $2\beta l$ into the reflection coefficient, which must be known in order to substitute the shorts reflection coefficient by $-1e^{-2\beta l}$. The same holds if offset shorts with electrical length $2\beta l$ are used. For a frequency band where $2\beta l$ is between 40° and 320°, the latter can replace the open standard, which typically suffers from fringing capacities and radiation losses. Therefore, the open standards contained in commercially available calibration kits come with detailed information on those imperfections, modeling the frequency dependence of the open's capacitance by a polynomial to enhance accuracy. For the absolute impedance reference, the Match standard, precision crafting is needed for precision measurements.

The 10-Term Error Model for Vector Network Analyzers with Three Receivers

For all practical purposes, the applicability of the five-term error model is somewhat impaired by the need for manually reversing the DUT in order to obtain error-corrected results. If a switch is incorporated into the VNA, as depicted in Fig. 11, this manual interaction can be automated, easing error-corrected measurements considerably.

In essence, the error model of the resulting bidirectional VNA with three receivers (see section entitled "The Three-Receiver Network Analyzer Architecture for Full Two-Port Measurements") consists of *two* five-term error models (Fig. 17). Because of the switch being located *between* m_1 and m_2 and m_1 and m_3, respectively, different error two-ports are needed for either position of the switch.

With the switch in position I, the reflectometer comprising m_1 and m_2 can be represented by an error two-port $[G^{\mathrm{I}}]$ and the reflectometer terminated in Z_0 and comprising m_3 by an error two-port $[H^{\mathrm{I}}]$. In the second state of the switch, the four-port comprising m_1 and m_3 can be reduced to the error two-port $[G^{\mathrm{II}}]$ and the reflectometer terminated in Z_0 and comprising m_2 by an error two-port $[H^{\mathrm{II}}]$ with

$$\begin{pmatrix} b_1 \\ a_1 \end{pmatrix} = [G^I] \begin{pmatrix} m_2^{\mathrm{I}} \\ m_1^{\mathrm{I}} \end{pmatrix}, \quad \begin{pmatrix} b_2 \\ a_2 \end{pmatrix} = [H^I] \begin{pmatrix} m_3^{\mathrm{I}} \\ 0 \end{pmatrix}$$
$$\begin{pmatrix} b_1 \\ a_1 \end{pmatrix} = [H^{II}] \begin{pmatrix} m_2^{\mathrm{II}} \\ 0 \end{pmatrix}, \begin{pmatrix} b_2 \\ a_2 \end{pmatrix} = [G^{II}] \begin{pmatrix} m_3^{\mathrm{II}} \\ m_1^{\mathrm{II}} \end{pmatrix}$$

Using these relations together with Eq. (14) yields a vector equation for either state of the switch which can be combined into a matrix equation, very similar to Eq. (16):

$$\begin{bmatrix} G_{11}^{\mathrm{I}} m_2^{\mathrm{I}} + G_{12}^{\mathrm{I}} m_1^{\mathrm{I}} & H_{11}^{\mathrm{II}} m_2^{\mathrm{II}} \\ H_{11}^{\mathrm{I}} m_3^{\mathrm{I}} & G_{11}^{\mathrm{II}} m_3^{\mathrm{II}} + G_{12}^{\mathrm{II}} m_1^{\mathrm{II}} \end{bmatrix} = [S] \begin{bmatrix} G_{21}^{\mathrm{I}} m_2^{\mathrm{I}} + G_{22}^{\mathrm{I}} m_1^{\mathrm{I}} & H_{21}^{\mathrm{II}} m_2^{\mathrm{II}} \\ H_{21}^{1} m_3^{\mathrm{I}} & G_{21}^{\mathrm{II}} m_3^{\mathrm{II}} + G_{22}^{\mathrm{II}} m_1^{\mathrm{II}} \end{bmatrix}$$

Figure 16. Calibration standards for the TMSO five-term procedure. Through: $[S^T] = \begin{bmatrix} 0 & 1 \\ 1 & 0 \end{bmatrix}$, Open: $S_{11}^O = 1$, Short: $S_{11}^S = -1$, Match: $S_{11}^M = 0$

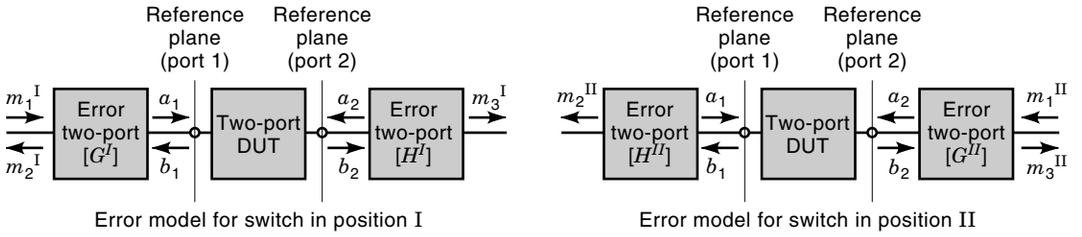

Figure 17. Error model of the bidirectional vector network analyzer with three receivers.

Normalization to the incident waves m_1^{I} and m_1^{II} now yields

$$\begin{bmatrix} G_{11}^{\mathrm{I}} m_{11} + G_{12}^{\mathrm{I}} & H_{11}^{\mathrm{II}} m_{12} \\ H_{11}^{\mathrm{I}} m_{21} & G_{11}^{\mathrm{II}} m_{22} + G_{12}^{\mathrm{II}} \end{bmatrix} = [S] \begin{bmatrix} G_{21}^{\mathrm{I}} m_{11} + G_{22}^{\mathrm{I}} & H_{21}^{\mathrm{II}} m_{12} \\ H_{21}^{\mathrm{I}} m_{21} & G_{21}^{\mathrm{II}} m_{22} + G_{22}^{\mathrm{II}} \end{bmatrix} \quad (19)$$

with

$$m_{11} = \frac{m_2^{\mathrm{I}}}{m_1^{\mathrm{I}}} = \frac{\eta_2 b_{m_2}}{\eta_1 b_{m_1}}, \quad m_{21} = \frac{m_3^{\mathrm{I}}}{m_1^{\mathrm{I}}} = \frac{\eta_3 b_{m_3}}{\eta_1 b_{m_1}}$$

$$m_{12} = \frac{m_2^{\mathrm{II}}}{m_1^{\mathrm{II}}} = \frac{\eta_2 b_{m_2}}{\eta_1 b_{m_1}}, \quad m_{22} = \frac{m_3^{\mathrm{II}}}{m_1^{\mathrm{II}}} = \frac{\eta_3 b_{m_3}}{\eta_1 b_{m_1}}$$

where comparison with the five-term error model shows that m_2^{II} and m_3^{II} have switched their position as have the error terms for the second state of the switch, a consequence of the switch now reversing the DUT and the error two-ports.

With error correction according to the 10-term error model applied, the requirements of the switch as detailed in the section entitled "The Three-Receiver Network Analyzer Architecture for Full Two-Port Measurements" become somewhat relaxed, because its mismatch errors and transmission losses are now accounted for. However, repeatability and leakage errors (finite isolation) are not contained in the error model.

Calibration of the 10-Term Error Model. As was the case with the five-term model, not all 16 error terms appear in Eq. (19). H_{12}^{I}, H_{22}^{I}, H_{12}^{II}, and H_{22}^{II} are not needed for error correction and cannot be determined by the calibration procedure.

Rearranging Eq. (19) as a linear homogeneous system of equations in the remaining error terms, as demonstrated in the section entitled "Calibration of the Five-Term Error Model," finds the four equations to be decoupled: Two equations depend solely upon error terms of $[G^{\mathrm{I}}]$ and $[H^{\mathrm{I}}]$, and the other two equations depend only upon $[G^{\mathrm{II}}]$ and $[H^{\mathrm{II}}]$:

$$\begin{bmatrix} -m_{11}^i & -1 & S_{11}^i m_{11}^i & S_{11}^i & 0 & S_{12}^i m_{21}^i \\ 0 & 0 & S_{21}^i m_{11}^i & S_{21}^i & -m_{21}^i & S_{22}^i m_{21}^i \end{bmatrix} \boldsymbol{e}^{\mathrm{I}} = 0,$$

$$\boldsymbol{e}^{\mathrm{I}} = (G_{11}^{\mathrm{I}}, G_{12}^{\mathrm{I}}, G_{21}^{\mathrm{I}}, G_{22}^{\mathrm{I}}, H_{11}^{\mathrm{I}}, H_{21}^{\mathrm{I}})^T$$

$$\begin{bmatrix} 0 & 0 & S_{12}^i m_{22}^i & S_{12}^i & -m_{12}^i & S_{11}^i m_{12}^i \\ -m_{22}^i & -1 & S_{22}^i m_{22}^i & S_{22}^i & 0 & S_{21}^i m_{12}^i \end{bmatrix} \boldsymbol{e}^{\mathrm{II}} = 0,$$

$$\boldsymbol{e}^{\mathrm{II}} = (G_{11}^{\mathrm{II}}, G_{12}^{\mathrm{II}}, G_{21}^{\mathrm{II}}, G_{22}^{\mathrm{II}}, H_{11}^{\mathrm{II}}, H_{21}^{\mathrm{II}})^T$$

With one of the error terms of both $\boldsymbol{e}^{\mathrm{I}}$ and $\boldsymbol{e}^{\mathrm{II}}$ set to 1 (e.g., $G_{11}^{\mathrm{I}} = G_{11}^{\mathrm{II}} = 1$), two sets of five independent equations must be supplied by the calibration measurements in order to solve the resulting inhomogeneous system for the remaining 10 error terms.

A similar reasoning (compared with the section entitled "Calibration of the Five-Term Error Model") as to how many and what kind of standards are needed is applicable here. At least one standard with transmission ($S_{21} \neq 0$ and $S_{12} \neq 0$) is needed in order to determine $[H^{\mathrm{I}}]$ and $[H^{\mathrm{II}}]$. Because of the different error terms, such a standard will supply a total of four equations for both positions of the switch. Reflection two-ports ($S_{21} = S_{12} = 0$), on the other hand, still contribute one equation for each of their two reflection coefficients S_{11} and S_{22}.

The same standards as with the five term error model (referred to as TMSO, Through-Match-Short-Open, or SOLT, Short-Open-Load-Through) are commonly used to calibrate the 10-term model, with the reflection standards now being reflection two-ports.

Because of the decoupled nature of Eq. (19), the reflection two-ports may be realized as one-ports by first connecting the calibration impedance to port 1 and noting the measurement values with the switch in position I. Then the appropriate calibration impedance is connected to port 2 and the measurements are taken with the switch in the second position [since these standards do not exhibit transmission, the corresponding transmission receiver (m_3^{I}, m_2^{II}) need not be considered]. With respect to the commonly used TMSO standards, this sequential procedure eliminates the need for two identical reflection standards but allows usage of one physical match—short and open—as reflection one-ports.

The Cross-Talk Including 12-Term Error Model for Three-Receiver VNAs

A number of commercially available VNAs provide a 12-term calibration capability (17), expanding the above-described 10-term error model by two error terms that characterize forward and reverse isolation. Their inclusion aims at extending the dynamic range for measurements where finite isolation of the switch or coupling over the DUT adversely affects measurement accuracy at high insertion loss levels of the DUT.

For that purpose an additional isolation standard (no transmission) with, for now, arbitrary reflection coefficients r_1 and r_2

$$[S^X] = \begin{bmatrix} r_1 & 0 \\ 0 & r_2 \end{bmatrix} \rightarrow [M^X] = \begin{bmatrix} m_{11}^X & m_{12}^X \\ m_{21}^X & m_{22}^X \end{bmatrix}$$

must be measured (alternatively the transmission measurement of one of the reflection standards may be exploited). The

transmission terms m_{12}^X and m_{21}^X of its measurement matrix are a measure of the cross-talk level and can be used for correcting the measured transmission values of the DUT:

$$[S] = \begin{bmatrix} G_{11}^{\mathrm{I}} m_{11} + G_{12}^{\mathrm{I}} & H_{11}^{\mathrm{II}}(m_{12} - m_{12}^X) \\ H_{11}^{\mathrm{I}}(m_{21} - m_{21}^X) & G_{11}^{\mathrm{II}} m_{22} + G_{12}^{\mathrm{II}} \end{bmatrix} \times \begin{bmatrix} G_{21}^{\mathrm{I}} m_{11} + G_{22}^{\mathrm{I}} & H_{21}^{\mathrm{II}}(m_{12} - m_{12}^X) \\ H_{21}^{\mathrm{I}}(m_{21} - m_{21}^X) & G_{21}^{\mathrm{II}} m_{22} + G_{22}^{\mathrm{II}} \end{bmatrix}^{-1}$$

However, this simple correction scheme can only improve results if the reflection coefficients of the isolation standard match the reflection coefficients of the DUT. For well-matched DUTs, the isolation terms can be taken from the measurement of the Match standard $[S^M]$. High transmission dynamic DUTs (e.g., filters), however, typically exhibit strongly varying reflection coefficients over frequency. If two identical DUTs are available, an isolation standard that satisfies the above condition can be generated by connecting the first DUT with port 1 to port 1 of the VNA and the second DUT with port 2 to the VNAs second port. The unused ports of the DUTs are terminated in Z_0. Consequently the isolation measurement must be repeated with a suitable isolation standard whenever DUTs with differing reflection coefficients are to be measured.

Considering the above limitations, the cross-talk reduction with the 12-term model should be regarded as a cross-talk *normalization* rather than a *calibration.*

In the section entitled "The Cross-Talk Correcting 15-Term Error Model for Four-Receiver VNAs," it will be shown that for an error model to correctly include cross-talk, eight error terms are needed for its characterization.

The Seven-Term Error Model for Vector Network Analyzers with Four Receivers

The addition of a fourth receiver to independently measure all four waves at the DUT, as depicted in Fig. 12, leads to very interesting instrument properties and calibration possibilities. The DUT is now embedded in a symmetrical test set, consisting of two reflectometers, each of which can be represented by an error two-port (see section entitled "The Three-Term Error Model for Reflection Measurements," which discusses four-port/two-port reduction).

The subtle but far-reaching advantages of this architecture and the accompanying error-model are:

1. The error model (Fig. 19) is valid for *either* position of the switch, reducing the number of error terms to eight and the number of two-port calibration standards required to three.

Through: $[S^T] = \begin{bmatrix} 0 & 1 \\ 1 & 0 \end{bmatrix}$, Open: $[S_{\mathrm{open}}^O] = \begin{bmatrix} 1 & 0 \\ 0 & 1 \end{bmatrix}$

Short: $[S^S] = \begin{bmatrix} -1 & 0 \\ 0 & -1 \end{bmatrix}$, Match: $[S^M] = \begin{bmatrix} 0 & 0 \\ 0 & 0 \end{bmatrix}$

Figure 18. Calibration standards for the TMSO (SOLT) 10-term procedure.

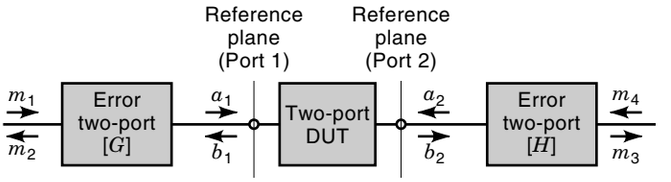

Figure 19. Seven-term error model of the bidirectional vector network analyzer with four receivers.

2. The four-receiver architecture provides redundant information in the calibration measurements that can be exploited to allow calibration with *partially unknown* standards. The section entitled "Modern Self-Calibration Techniques for Four-Receiver VNAs" details these important and powerful techniques.
3. The switch is no longer part of the error two-ports. Instead it has been moved into the generator port of the reflectometers, whose waves were eliminated during the four-port/two-port reduction. Therefore, the imperfections of the switch no longer influence the quality of an error-corrected measurement. The switch may be mismatched, may exhibit transmission losses and finite isolation, and does not even need to be repeatable.

The mathematical derivation of the seven-term error model unfolds in the usual way. With

$$\begin{pmatrix} b_1 \\ a_1 \end{pmatrix} = [G] \begin{pmatrix} m_2 \\ m_1 \end{pmatrix}, \quad \begin{pmatrix} b_2 \\ a_2 \end{pmatrix} = [H] \begin{pmatrix} m_3 \\ m_4 \end{pmatrix}, \quad \text{and} \quad \begin{pmatrix} b_1 \\ b_2 \end{pmatrix} = [S] \begin{pmatrix} a_1 \\ a_2 \end{pmatrix} \tag{20}$$

vector equations for both positions of the switch (I and II) are obtained and combined into a matrix equation:

$$\begin{bmatrix} G_{11} m_2^{\mathrm{I}} + G_{12} m_1^{\mathrm{I}} & G_{11} m_2^{\mathrm{II}} + G_{12} m_1^{\mathrm{II}} \\ H_{11} m_3^{\mathrm{I}} + H_{12} m_4^{\mathrm{I}} & H_{11} m_3^{\mathrm{II}} + H_{12} m_4^{\mathrm{II}} \end{bmatrix} = [S] \begin{bmatrix} G_{21} m_2^{\mathrm{I}} + G_{22} m_1^{\mathrm{I}} & G_{21} m_2^{\mathrm{II}} + G_{22} m_1^{\mathrm{II}} \\ H_{21} m_3^{\mathrm{I}} + H_{22} m_4^{\mathrm{I}} & H_{21} m_3^{\mathrm{II}} + H_{22} m_4^{\mathrm{II}} \end{bmatrix} \tag{21}$$

The eight measurement values contained in Eq. (21) can be condensed to four by expanding Eq. (21) as

$$\begin{bmatrix} G_{12} & 0 \\ 0 & H_{12} \end{bmatrix} \begin{bmatrix} m_1^{\mathrm{I}} & m_1^{\mathrm{II}} \\ m_4^{\mathrm{I}} & m_4^{\mathrm{II}} \end{bmatrix} + \begin{bmatrix} G_{11} & 0 \\ 0 & H_{11} \end{bmatrix} \begin{bmatrix} m_2^{\mathrm{I}} & m_2^{\mathrm{II}} \\ m_3^{\mathrm{I}} & m_3^{\mathrm{II}} \end{bmatrix} = [S] \left\{ \begin{bmatrix} G_{22} & 0 \\ 0 & H_{22} \end{bmatrix} \begin{bmatrix} m_1^{\mathrm{I}} & m_1^{\mathrm{II}} \\ m_4^{\mathrm{I}} & m_4^{\mathrm{II}} \end{bmatrix} + \begin{bmatrix} G_{21} & 0 \\ 0 & H_{21} \end{bmatrix} \begin{bmatrix} m_2^{\mathrm{I}} & m_2^{\mathrm{II}} \\ m_3^{\mathrm{I}} & m_3^{\mathrm{II}} \end{bmatrix} \right\}$$

and right-multiplying both sides with the inverse measurement matrix of the first and fourth receiver. The result is much simplified error-model representation

$$\begin{bmatrix} G_{12} & 0 \\ 0 & H_{12} \end{bmatrix} + \begin{bmatrix} G_{11} & 0 \\ 0 & H_{11} \end{bmatrix} [M] = [S] \left\{ \begin{bmatrix} G_{22} & 0 \\ 0 & H_{22} \end{bmatrix} + \begin{bmatrix} G_{21} & 0 \\ 0 & H_{21} \end{bmatrix} [M] \right\} \tag{22}$$

with a 2×2 measurement matrix

$$[M] = \begin{bmatrix} m_2^{\mathrm{I}} & m_2^{\mathrm{II}} \\ m_3^{\mathrm{I}} & m_3^{\mathrm{II}} \end{bmatrix} \begin{bmatrix} m_1^{\mathrm{I}} & m_1^{\mathrm{II}} \\ m_4^{\mathrm{I}} & m_4^{\mathrm{II}} \end{bmatrix}^{-1} = \begin{bmatrix} m_{11} & m_{12} \\ m_{21} & m_{22} \end{bmatrix}$$

With the measurement values pertaining to the incident waves m_1^{I} and m_4^{II} residing on the main diagonal of the right submatrix and the off-diagonal elements being small, the matrix is guaranteed to be invertible. For $m_4^{\mathrm{I}} = m_1^{\mathrm{II}} = 0$ (three receiver analogy) the entries of $[M]$ are normalized with respect to the incident waves m_1^{I} and m_4^{II}. The measurement matrix $[M]$ is therefore attributed S-parameter character. Furthermore, the computation of $[M]$ provides a first level of error correction, because finite isolation of the switch is eliminated. This is achieved by the fourth receiver, which precisely measures the level of the switch's leakage signals through m_1^{II} and m_4^{I}.

Equation (22) is easily returned to the structure of Eq. (21), with the four measurement values now being direct counterparts of the corresponding error-corrected S-parameters of the DUT:

$$\begin{bmatrix} G_{11}m_{11} + G_{12} & G_{11}m_{12} \\ H_{11}m_{21} & H_{11}m_{22} + H_{12} \end{bmatrix} = [S] \begin{bmatrix} G_{21}m_{11} + G_{22} & G_{21}m_{12} \\ H_{21}m_{21} & H_{21}m_{22} + H_{22} \end{bmatrix} \quad (23)$$

It may be interesting to note that $[G]$ and $[H]$ are of the cascading *transfer matrix* type. This type of matrix also appears in all the other error models introduced in this section. The fact that transfer matrices exhibit a singularity if the underlying network has zero transmission can safely be ignored as far as error two-ports of practical reflectometer or network analyzer realizations are concerned. Those networks *must* exhibit transmission in order to perform the desired function. The device under test, however, may be perfectly isolating and should therefore always be represented by its S-matrix (the section entitled "The General TAN Procedure" introduces *pseudo-transfer matrices* to work around that singularity).

Calibration of the Seven-Term Error Model. With Eq. (23) being of the same structure as the five-term model [Eq. (16)] and the 10-term model [Eq. (19)], the determination of the error terms proceeds in the same way. Equation (23) is rearranged into a linear homogeneous system of equations

$$\begin{bmatrix} -m_{11}^i & -1 & S_{11}^i m_{11}^i & S_{11}^i & 0 & 0 & S_{12}^i m_{21}^i & 0 \\ 0 & 0 & S_{21}^i m_{11}^i & S_{21}^i & -m_{21}^i & 0 & S_{22}^i m_{21}^i & 0 \\ -m_{12}^i & 0 & S_{11}^i m_{12}^i & 0 & 0 & 0 & S_{12}^i m_{22}^i & S_{12}^i \\ 0 & 0 & S_{21}^i m_{12}^i & 0 & -m_{22}^i & -1 & S_{22}^i m_{22}^i & S_{22}^i \end{bmatrix} \boldsymbol{e} = 0,$$

$$\boldsymbol{e} = (G_{11}, \ldots, G_{22}, H_{11}, \ldots, H_{22})^T$$

with every calibration measurement i contributing four equations. One error term is set to 1, and seven independent equations are required to solve for the remaining seven error terms. It turns out that the eight equations stemming from the measurement of two calibration two-ports are not sufficient to provide the necessary rank of 7. Measurement of a third calibration two-port is needed such that a total of 12 equations exist.

The resulting surplus in information can be used in one of the following ways:

1. The linear system with all 12 equations is solved in the least-squares sense (e.g., see Ref. 19), using the extra equations to minimize residual errors (contacting or repeatability errors).
2. Even though contacting errors cannot be accounted for due to their statistical nature, in Ref. 20 the extra information is used to assess these errors by deriving error bounds. As these techniques are not yet widely used, they will not be further treated here.
3. The calibration standards can be permitted to have unknown parameters (13,21), which are determined using the extra information contained in the additional equations. Because the construction of standards, which do not have to be fully known, can result in considerable savings, this "self-calibration" technique is of much practical importance. The section entitled "Modern Self-Calibration Techniques for Four-Receiver VNAs" has the details.

Performing a seven-term calibration with completely known standards is most easily done using the TMS procedure, where the three calibration two-ports

$$\text{Through:} \quad [S^T] = \begin{bmatrix} 0 & 1 \\ 1 & 0 \end{bmatrix}, \quad \text{Match:} \quad [S^M] = \begin{bmatrix} 0 & 0 \\ 0 & 0 \end{bmatrix}$$

$$\text{Short:} \quad [S^S] = \begin{bmatrix} -1 & 0 \\ 0 & -1 \end{bmatrix}$$

are used. Comparison with the 10-term and the 5-term model shows that the third reflection standard is no longer needed. Using a short, instead of an open, as the third standard is in many cases the more convenient choice, because shorts can be manufactured to higher precision in coaxial media or waveguides (see section entitled "Calibration of the Five-Term Error Model"). At low frequencies, however, using an open may be the more advantageous choice, as the test port itself serves as a comparatively good open up to about 100 MHz.

The computed error terms are used for error correction by simply solving Eq. (23) for $[S]$:

$$[S] = \begin{bmatrix} G_{11}m_{11} + G_{12} & G_{11}m_{12} \\ H_{11}m_{21} & H_{11}m_{22} + H_{12} \end{bmatrix} \times \begin{bmatrix} G_{21}m_{11} + G_{22} & G_{21}m_{12} \\ H_{21}m_{21} & H_{21}m_{22} + H_{22} \end{bmatrix}^{-1}$$

Calibration of the Seven-Term Error Model using an Unknown Through. For applications where a *T*hrough standard of known properties is not available, the seven-term error model may be calibrated by performing simple reflectometer calibrations for the error two-ports $[G]$ and $[H]$, according to the section entitled "Calibration of the Three-Term Error Model," and using a transmission standard whose only known property is its reciprocity (e.g., $S_{21} = S_{12}$).

Such a calibration method may, for instance, be desirable for on-wafer measurements where nonaligned measurement ports render a known Through difficult to build (22). Calibra-

tion without an unknown Through was first introduced in Ref. 23 and is very simple to derive if the cascade structure of the error model (Fig. 19) is written using transfer matrices. With the error two-ports [G] and [H] already in that notation [Eq. (20)], the difference to Eq. (22) is in the description of the DUT

$$\begin{pmatrix} b_1 \\ a_1 \end{pmatrix} = [\Sigma] \begin{pmatrix} a_2 \\ b_2 \end{pmatrix} = \frac{1}{S_{21}} \begin{bmatrix} -\Delta S & S_{11} \\ -S_{22} & 1 \end{bmatrix} \begin{pmatrix} a_2 \\ b_2 \end{pmatrix} \tag{24}$$

and in the evolving measurement matrix

$$\begin{bmatrix} m_1^{\mathrm{I}} & m_1^{\mathrm{II}} \\ m_2^{\mathrm{I}} & m_2^{\mathrm{II}} \end{bmatrix} \begin{bmatrix} m_3^{\mathrm{I}} & m_3^{\mathrm{II}} \\ m_4^{\mathrm{I}} & m_4^{\mathrm{II}} \end{bmatrix}^{-1} = [P] = [G]^{-1}[\Sigma][H]$$

with the latter now also being a transfer matrix.

Performing reflectometer calibrations, as described in the section entitled "Calibration of the Three-Term Error Model," for both error two-ports establishes three of the four error terms in [G] and [H], leading to the preliminary error matrices [$\tilde{G}$] and [$\tilde{H}$], with one error term normalized to 1. Without loss of generality, let us assume $\tilde{G}_{11} = \tilde{H}_{11} = 1$. This knowledge of [$G$] and [$H$], except for a common factor, can be expressed as

$$[P] = [G]^{-1}[\Sigma][H] = \frac{1}{K_G}[\tilde{G}]^{-1}[\Sigma]K_H[\tilde{H}] = \alpha[\tilde{G}]^{-1}[\Sigma][\tilde{H}]$$

$$\alpha = \frac{K_H}{K_G}$$

The still unknown term α can be regarded as the seventh error term, still needed for a full two-port calibration. As the determinant of the transfer matrix of a reciprocal two-port is unity, using such a device for calibration produces the equation

$$\det[P^{\mathrm{reci}}] = \alpha^2 \det[\tilde{G}]^{-1} \det[\Sigma^{\mathrm{reci}}] \det[\tilde{H}] = \alpha^2 \frac{\det[\tilde{H}]}{\det[\tilde{G}]}$$

which is solved for α:

$$\alpha = \pm\sqrt{\frac{\det[\tilde{G}]}{\det[\tilde{H}]}\det[P^{\mathrm{reci}}]} \tag{25}$$

According to Ref. 23, the correct root in Eq. (25) is most easily found using

$$S_{21}^{\mathrm{reci}} = \frac{\alpha}{P_{22}^{\mathrm{reci}}}$$

if the phase of the reciprocal transmission-factor is known to $\pm 90°$.

The Cross-Talk Correcting 15-Term Error Model for Four-Receiver VNAs

Whenever energy emanating from the measurement planes finds a path to leak around the DUT or a coupling path between the reflectometers of the VNA exists (Fig. 20), the error models of the sections entitled "The Five-Term Error Model for Unidirectional Vector Network Analyzers," "The 10-Term Error Model for Vector Framework Analyzers with Three Receivers," "The Cross-Talk Including 12-Term Error Model for Three-Receiver VNAs," and "The Seven-Term Error Model for Vector Network Analyzers with Four Receivers" cannot adequately handle the associated cross-talk error. On-wafer measurements typically suffer from this kind of leakage error, due to the small separation of the measurement planes and the radiation of the probe tips.

An error model, capable of accounting for those leakage errors was first detailed in Ref. 24 and is also termed *full-model* (14). It can be derived by describing the four-receiver VNA's hardware as a general eight-port. The coupling between the reflectometers may be arbitrary and nonreciprocal but must be linear and not affected by the parameters of the DUT. Comparable to the four-port/two-port reduction, introduced in the section entitled "Calibration of the Five-Term Error Model," the reflection coefficients and conversion constants of the four receivers are used to eliminate the reflected waves at the receivers and the generator waves a_G and b_G.

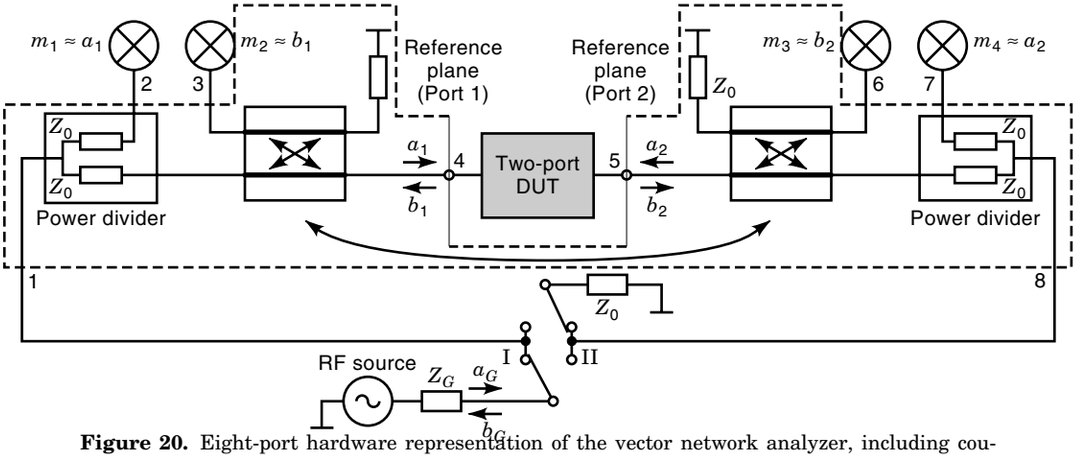

Figure 20. Eight-port hardware representation of the vector network analyzer, including coupling of the reflectometers.

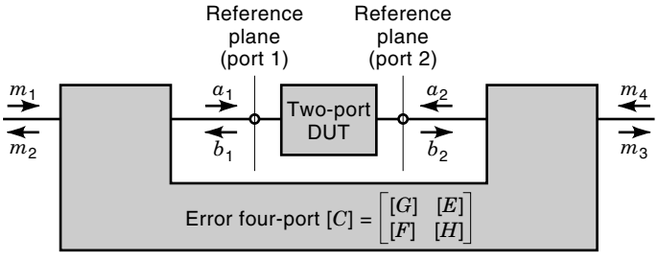

Figure 21. Fifteen-term error-model of the four-receiver vector network analyzer.

The resulting error four-port $[C]$ (Fig. 21) relates the measured values $m_i\,(i = 1, 2, 3, 4)$ to the waves a_1, a_2, b_1, b_2 at the DUT such that its S-matrix can be computed from the measurement data and $[C]$. Because the switch is not part of the error network and the waves of the RF source are eliminated in Eq. (26), the properties of the switch have no influence on the quality of error correction, and the same error network may be used for either state of the switch.

The mathematical formulation of the error model is derived by partitioning the 4×4 matrix $[C]$ into four 2×2 matrices. With

$$\begin{pmatrix} b_1 \\ b_2 \\ a_1 \\ a_2 \end{pmatrix} = [C] \begin{pmatrix} m_1 \\ m_4 \\ m_2 \\ m_3 \end{pmatrix} = \begin{bmatrix} [G] & [E] \\ [F] & [H] \end{bmatrix} \begin{pmatrix} m_1 \\ m_4 \\ m_2 \\ m_3 \end{pmatrix} \tag{26}$$

the two vector equations

$$\begin{pmatrix} b_1 \\ b_2 \end{pmatrix} = [G] \begin{pmatrix} m_1 \\ m_4 \end{pmatrix} + [E] \begin{pmatrix} m_2 \\ m_3 \end{pmatrix}$$

$$\begin{pmatrix} a_1 \\ a_2 \end{pmatrix} = [F] \begin{pmatrix} m_1 \\ m_4 \end{pmatrix} + [H] \begin{pmatrix} m_2 \\ m_3 \end{pmatrix}$$

can be derived to express the waves at the DUT as

$$[G] \begin{pmatrix} m_1 \\ m_4 \end{pmatrix} + [E] \begin{pmatrix} m_2 \\ m_3 \end{pmatrix} = [S] \left\{ [F] \begin{pmatrix} m_1 \\ m_4 \end{pmatrix} + [H] \begin{pmatrix} m_2 \\ m_3 \end{pmatrix} \right\}$$

An equation of this type is obtained for measurement in either position of the switch, and combining both vector equations into a matrix equation yields

$$[G] \begin{bmatrix} m_1^{\mathrm{I}} & m_1^{\mathrm{II}} \\ m_4^{\mathrm{I}} & m_4^{\mathrm{II}} \end{bmatrix} + [E] \begin{bmatrix} m_2^{\mathrm{I}} & m_2^{\mathrm{II}} \\ m_3^{\mathrm{I}} & m_3^{\mathrm{II}} \end{bmatrix} = [S] \left\{ [F] \begin{bmatrix} m_1^{\mathrm{I}} & m_1^{\mathrm{II}} \\ m_4^{\mathrm{I}} & m_4^{\mathrm{II}} \end{bmatrix} + [H] \begin{bmatrix} m_2^{\mathrm{I}} & m_2^{\mathrm{II}} \\ m_3^{\mathrm{I}} & m_3^{\mathrm{II}} \end{bmatrix} \right\}$$

which simplifies to

$$[G] + [E][M] = [S]\{[F] + [H][M]\} \tag{27}$$

by introduction of the measurement matrix

$$[M] = \begin{bmatrix} m_2^{\mathrm{I}} & m_2^{\mathrm{II}} \\ m_3^{\mathrm{I}} & m_3^{\mathrm{II}} \end{bmatrix} \begin{bmatrix} m_1^{\mathrm{I}} & m_1^{\mathrm{II}} \\ m_4^{\mathrm{I}} & m_4^{\mathrm{II}} \end{bmatrix}^{-1} = \begin{bmatrix} m_{11} & m_{12} \\ m_2 & m_{22} \end{bmatrix}$$

Comparison with the formulation of the seven-term model [Eq. (22)] reveals the very close relationship, because their structure and even the measurement matrix are identical. In fact, the seven-term error model evolves as a special case of the more general 15-term model. Consequently, the eight off-diagonal error terms that default to zero in Eq. (21), where no leakage is assumed, are needed in the 15-term model to correctly describe the cross-talk.

Calibration of the 15-Term Error Model. Determination of the 16 error terms in the error quadrants $[G]$, $[E]$, $[F]$, and $[H]$ is achieved by expanding Eq. (27) into a system of four linear equations in the error terms per calibration measurement (25). One error term may be arbitrarily set to one, and the resulting inhomogeneous system may be solved for the remaining 15 error terms. Care must be taken to choose one of the error terms *on* the diagonal of the error-quadrants for this normalization, because the *off*-diagonal elements vanish in the case of a leakage-free error four-port.

It turns out that at least five completely known and distinct calibration two-ports must be measured to determine the 15 error terms (25,26). With five calibration measurements, 20 equations in the 15 unknowns exist, but only 15 are needed. Analogous to the section entitled "The Seven-Term Model for Vector Network Analyzers with Four Receivers" either five suitable equations may be neglected or, alternatively, the system of 20 equations in 15 unknowns is solved in the least-squares sense. Use of partially unknown standards and their determination through self-calibration is the third option and is outlined in the section entitled "Self-Calibration for the 15-Term Error Model."

An especially well-suited combination of standards for the 15-term model, first mentioned in Ref. 25, consists of a Through two-port and the three reflection one-ports *m*atch, *s*hort, and *o*pen, combined to yield four reflection two-ports such that calibration is performed with the five two-ports of Fig. 22.

Contrary to the 7-term, 5-term, or 10-term error-models, the 15-term model does not allow reflection two-ports to be measured sequentially, by separating the reflection measurements at both ports. Due to the presence of cross-talk that must be precisely measured, both ports need to be terminated in the prescribed impedance while performing the calibration measurement. Cyclically interchanging the three reflection one-ports to create the calibration standard lets this Tmso procedure get by with one match-, short-, and open standard. Lowercase letters are used to indicate that match, short, and open are one-ports and need to be combined to form the necessary calibration two-ports.

Once all error terms are known, the measured values of an arbitrary DUT are to be error-corrected. Contrary to the calibration process, error correction is performed with every measurement. Numerical efficiency is therefore in demand.

Equation (27) is easily solved for the S-matrix $[S]$ of the DUT

$$[S] = \{[G][M] + [E]\}\{[H][M] + [F]\}^{-1}$$

and devises a very simple algorithm for the error-correction process. Only 2×2 matrices need to be manipulated.

Figure 23 (taken from Ref. 27) demonstrates the capabilities of the 15-term procedure in the presence of an artificial

Figure 22. Calibration standards for the 15-term Tmso-procedure.

$$S^{T} = \begin{bmatrix} 0 & 1 \\ 1 & 0 \end{bmatrix}, \quad S^{MS} = \begin{bmatrix} 0 & 0 \\ 0 & -1 \end{bmatrix}, \quad S^{OM} = \begin{bmatrix} 1 & 0 \\ 0 & 0 \end{bmatrix}, \quad S^{SO} = \begin{bmatrix} -1 & 0 \\ 0 & 1 \end{bmatrix}, \quad S^{OS} = \begin{bmatrix} 1 & 0 \\ 0 & -1 \end{bmatrix}$$

leakage error between the measurement planes. Figure 24 depicts the setup. The DUT is a 20 dB attenuator, and the cross-talk is modeled by a second 20 dB attenuator in parallel to the DUT.

While the presence of the leakage error corrupts the result in a way that the uncorrected data bears no resemblance with the transfer characteristics of the DUT, correcting the data according to the 15-term procedure recovers the attenuation value with good precision, even though the amount of cross-talk is of the same magnitude as the DUT's transmission.

MODERN SELF-CALIBRATION TECHNIQUES FOR FOUR-RECEIVER VNAs

Calibration of four-receiver VNAs according to the 7-term or the 15-term error model yields five redundant equations that are not needed for the computation of the error terms. Using this extra information for the determination of unknown parameters of the calibration standards is a very powerful technique that allows the calibration to be performed with *partially known* standards. Besides reducing the cost of standards, self-calibration techniques also enhance the accuracy of the calibration as inconsistency errors are reduced.

One of the most popular self-calibration representative, introduced in 1979 by Engen and Hoer (13) for the double six-port reflectometer (seven-term error model), is the TLR procedure. It allows calibration with the following standards:

- (T)hrough (direct connection of both measurement planes)
- (L)ine (a line of unknown electrical length, between 20° and 160°, perfectly matched)
- (R)eflect (unknown, but symmetrical reflection standard)

The L standard and the R standard are only partially known, with no requirements imposed upon the reflect, except that the same reflect has to be used on both measurement planes. Its value and the exact electrical length of the line are determined through the self-calibration process. Different methods can be employed for the determination of the unknown parameters of the standards, three of which are as follows:

1. The *linear* system of equations in the error terms [Eqs. (23) and (27)] is treated as a *nonlinear* system in the error terms *and* the unknowns of the standards. This nonlinear system is solved iteratively (28) or, where possible, analytically, providing a simultaneous solution of error terms and unknowns of the standards (17,18,29).
2. For a unique solution of the error terms to exist, five of the 12 (respectively 20) equations must be linearly dependent. If the 12×8 (20×16) coefficient matrix of the homogeneous linear system of equations [Eqs. (23) and (27)] can be *analytically* brought to tridiagonal form, the last five lines are required to vanish, resulting in five equations in which only measurement values and parameters of the standards appear. It may be argued that the analytical reduction of a 20×16 or even a 12×8 matrix to tridiagonal form is impracticable. However, Eqs. (23) and (27) are sparse enough to render the derivation of self-calibration equations according to this scheme feasible, even for the 15-term error model (30). Once the unknown parameters of the standards are determined, the standards are completely known and so are all nonzero entries of the tridiagonal matrix, which is then used to compute the error terms by a backsubstitution process (19, p. 37).
3. The formulation of the error model is rearranged to yield relations between the standards' S-parameters and the measured values, eliminating the error terms. These relations are exploited to solve for the unknown parameters of the calibration standards which are then completely known and can be used to solve the linear system of equations [Eqs. (23) and (27)] for the error terms. In the following sections, this method, which is based on similarity transformations (21,27), will be presented for the 7-term and the 15-term error model.

Self-Calibration for the Seven-Term Error Model

Elimination of the error parameters to arrive at a relation between the standards' parameters and the measurement values was first described by Eul and Schiek (21) and is most easily achieved by using transfer parameters to describe the cascade structure of the error model (Fig. 19). See Eq. (24) in

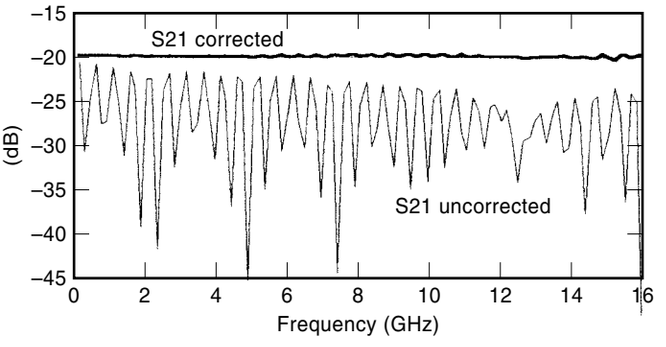

Figure 23. Transmission measurement of a 20 dB attenuator (corrected/uncorrected). (From Ref. 27, with permission.)

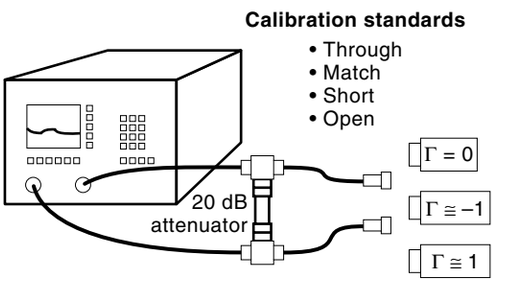

Figure 24. Measurement setup of a network analyzer with artificial cross-talk.

the section entitled "Calibration of the Seven-Term Error Model Using an Unknown Through."

As transfer parameters exhibit a singularity for transmissionless two-ports ($S_{21} = 0$), this representation of the error model is less suited for the computation of the error terms, which is why the S-parameter representation [Eq. (22)] was chosen in the section entitled "The Seven-Term Error Model for Vector Network Analyzers with Four Receivers." The seven-term error model, however, may as well be written using Eq. (24) with the three calibration measurements yielding three such equations.

Solving the ith calibration measurement for $[H]$.

$$[H] = [\Sigma_i]^{-1}[G][P_i]^{-1} \tag{28}$$

and substituting Eq. (28) into the remaining calibration measurements j and k yields

$$\begin{aligned} [P_j][P_i]^{-1} &= [G]^{-1}[\Sigma_j][\Sigma_i]^{-1}[G] \quad \text{and} \\ [P_k][P_i]^{-1} &= [G]^{-1}[\Sigma_k][\Sigma_i]^{-1}[G] \end{aligned} \tag{29}$$

Recognizing Eq. (29) as similarity transformations, the equality of the eigenvalues of the similar matrices is equivalent to the equality of their determinants and traces, hence

$$\begin{aligned} [\mathrm{A}] = [\mathrm{X}][\mathrm{B}][\mathrm{X}]^{-1} &\Rightarrow \det[\mathrm{A}] = \det[\mathrm{B}] \\ \mathrm{trace}[\mathrm{A}] = a_{11} + a_{22} &= \mathrm{trace}[\mathrm{B}] = b_{11} + b_{22} \end{aligned}$$

which yields the four equations

$$\begin{aligned} \det\{[P_j][P_i]^{-1}\} &= \beta_1 = \det\{[\Sigma_j][\Sigma_i]^{-1}\}, \\ \mathrm{trace}\{[P_j][P_i]^{-1}\} &= \beta_2 = \mathrm{trace}\{[\Sigma_j][\Sigma_i]^{-1}\} \\ \det\{[P_k][P_i]^{-1}\} &= \beta_3 = \det\{[\Sigma_k][\Sigma_i]^{-1}\}, \\ \mathrm{trace}\{[P_k][P_i]^{-1}\} &= \beta_4 = \mathrm{trace}\{[\Sigma_k][\Sigma_i]^{-1}\} \end{aligned} \tag{30}$$

The combination of both equations in Eq. (29) leads to a fifth condition for the standards' parameters:

$$\mathrm{trace}\{[P_j][P_i]^{-1}[P_k][P_i]^{-1}\} = \beta_5 = \mathrm{trace}\{[\Sigma_j][\Sigma_i]^{-1}[\Sigma_k][\Sigma_i]^{-1}\} \tag{31}$$

These five equations in Eqs. (30) and (31), in which only the transfer parameters of the standards and measurement values appear, can be used to compute a maximum of five unknown parameters of the standards.

The General TAN Procedure. One possibility to distribute the five unknowns among the three calibration standards is the general TAN procedure, where a Through standard (of known transmission factor t), a well-matched Attenuator (with unknown forward and reverse attenuation k_f and k_r), and a symmetrical, but not necessarily reciprocal, Network standard (with unknown reflection r and unknown transmission coefficients u_f and u_r) are used for calibration:

$$[\Sigma_T] = \begin{bmatrix} t & 0 \\ 0 & 1/t \end{bmatrix}, \quad [\Sigma_A] = \begin{bmatrix} k_r & 0 \\ 0 & 1/k_f \end{bmatrix}$$

$$[\Sigma_N] = \tfrac{1}{u_f}\begin{bmatrix} u_f u_r - r^2 & r \\ -r & 1 \end{bmatrix}$$

The inclusion of the known parameter t is for convenience if connector sex dictates the use of a nonzero length Through.

Since the A-standard may also turn into a well-matched Line standard (L) with $k_f = k_r = e^{-\gamma l}$, or into a double Match standard (M) with $k_f = k_r = 0$, and since the N standard may degenerate to a Reflection standard (R) with $u_f = u_r = 0$, the general TAN procedure also covers the most popular TLR and TMR self-calibration procedures.

However, the singularity of the transfer matrices $[\Sigma_A]$ and $[\Sigma_N]$ and the accompanying measurement matrices $[P_A]$ and $[P_N]$ for the case of vanishing transmission (M, R standard) must be taken care of. For that purpose, pseudo-transfer matrices are introduced (31) by separating the matrix of the measured quantities $[P]$ from its determinant Δm, which may be zero. The residual part of the matrix is denoted $[\tilde{P}]$

$$[P] = \begin{bmatrix} m_1^{\mathrm{I}} & m_1^{\mathrm{II}} \\ m_2^{\mathrm{I}} & m_2^{\mathrm{II}} \end{bmatrix} \frac{1}{m_3^{\mathrm{I}} m_4^{\mathrm{II}} - m_3^{\mathrm{II}} m_4^{\mathrm{I}}} \begin{bmatrix} m_4^{\mathrm{II}} & -m_3^{\mathrm{II}} \\ -m_4^{\mathrm{I}} & m_3^{\mathrm{I}} \end{bmatrix} = \frac{1}{\Delta m}[\tilde{P}] \tag{32}$$

with

$$\Delta m = m_3^{\mathrm{I}} m_4^{\mathrm{II}} - m_3^{\mathrm{II}} m_4^{\mathrm{I}} \quad \text{and} \quad [\tilde{P}] = \begin{bmatrix} m_1^{\mathrm{I}} & m_1^{\mathrm{II}} \\ m_2^{\mathrm{I}} & m_2^{\mathrm{II}} \end{bmatrix} \begin{bmatrix} m_4^{\mathrm{II}} & -m_3^{\mathrm{II}} \\ -m_4^{\mathrm{I}} & m_3^{\mathrm{I}} \end{bmatrix}$$

Combination of the determinant of the measurement matrix with the transfer matrix of the standard belonging to it yields the pseudo-transfer matrices

$$\begin{aligned} \Delta m_A[\Sigma_A] &= \frac{\Delta m_A}{k_f}\begin{bmatrix} k_r k_f & 0 \\ 0 & 1 \end{bmatrix} = \begin{bmatrix} \kappa_r & 0 \\ 0 & 1/\kappa_f \end{bmatrix} = [\Sigma_A^p] \\ \Delta m_N[\Sigma_N] &= \frac{\Delta m_N}{u_f}\begin{bmatrix} u_f u_r - r^2 & r \\ -r & 1 \end{bmatrix} = \frac{1}{\mu_f}\begin{bmatrix} \mu_f \mu_r - \rho^2 & \rho \\ -\rho & 1 \end{bmatrix} \\ &= [\Sigma_N^p] \end{aligned}$$

with

$$\begin{aligned} \kappa_f &= \frac{k_f}{\Delta m_A}, \quad \kappa_r = k_r \Delta m_A, \\ \mu_f &= \frac{u_f}{\Delta m_N}, \quad \mu_r = r_r \Delta m_N, \quad \rho = r \end{aligned} \tag{33}$$

and modifies Eqs. (30) and (31) as

$$\begin{aligned} \det\{[\tilde{P}_A][P_T]^{-1}\} &= \beta_1 = \det\{\Delta m_A[\Sigma_A][\Sigma_T]^{-1}\} \\ &= \det\{[\Sigma_A^p][\Sigma_T]^{-1}\} \\ \mathrm{trace}\{[\tilde{P}_A][P_T]^{-1}\} &= \beta_2 = \mathrm{trace}\{\Delta m_A[\Sigma_A][\Sigma_T]^{-1}\} \\ &= \mathrm{trace}\{[\Sigma_A^p][\Sigma_T]^{-1}\} \\ \det\{[\tilde{P}_N][P_T]^{-1}\} &= \beta_3 = \det\{\Delta m_N[\Sigma_N][\Sigma_T]^{-1}\} \\ &= \det\{[\Sigma_N^p][\Sigma_T]^{-1}\} \\ \mathrm{trace}\{[\tilde{P}_N][P_T]^{-1}\} &= \beta_4 = \mathrm{trace}\{\Delta m_N[\Sigma_N][\Sigma_T]^{-1}\} \\ &= \mathrm{trace}\{[\Sigma_N^p][\Sigma_T]^{-1}\} \\ \mathrm{trace}\{[\tilde{P}_A][P_T]^{-1}[\tilde{P}_N][P_T]^{-1}\} &= \beta_5 \\ &= \mathrm{trace}\{[\Sigma_A^p][\Sigma_T]^{-1}[\Sigma_N^p][\Sigma_T]^{-1}\} \end{aligned} \tag{34}$$

Because at least one standard must exhibit transmission, this property is, without loss of generality, attributed to the T standard, which therefore may be represented by a regular transfer matrix.

With β_i being nonsingular complex values, computed from the measurement values of the four receivers, according to Eq. (32), the first two equations of Eq. (34) can be used to determine the transmission coefficients of the A standard,

$$\frac{\kappa_r}{\kappa_f} = \beta_1, \quad \frac{\kappa_r}{t} + \frac{t}{\kappa_f} = \beta_2$$

which compute as

$$\kappa_r = t\left(\frac{\beta_2}{2} \pm \sqrt{\frac{\beta_2^2}{4} - \beta_1}\right) \quad \text{and} \quad \kappa_f = \frac{\kappa_r}{\beta_1} = \frac{t^2}{t\beta_2 - \kappa_r} \tag{35}$$

Similarly, the other parameters may be derived from the remaining equations in Eqs. (34) as

$$\mu_f = \frac{t^2 - \kappa_f\kappa_r}{t\kappa_f(\beta_5 - \kappa_r\beta_4)}, \quad \mu_r = \mu_f\beta_3 \tag{36}$$

$$\rho = \pm\sqrt{\mu_f\mu_r - \frac{\beta_4\mu_f}{t} + \frac{1}{t^2}} \tag{37}$$

Using Eq. (33), the parameters of the transfer matrices of the standards $[\Sigma_A]$ and $[\Sigma_N]$ are computed from the above-derived pseudo-transfer parameters.

The root ambiguity in Eq. (35) is solved with a priori knowledge of the A standard's transmission factor. If the standard exhibits attenuation ($|k_r| < 1$), the root whose magnitude is below 1 will be chosen, since the standard is passive. If a line standard with $|k_f| = |k_r| \approx 1$ is used, the phase of the line's transmission factor must be known to $\pm 90°$ in order to select the correct root.

The root choice in Eq. (37) requires the same kind of information about the phase of the N standard's reflection coefficient, which must be known to $\pm 90°$.

Equations (35) to (37) allow the computation of the calibration standards for the general TAN calibration procedure, also accounting for the special cases of the TMN, TMR, TAR, TLN, and TLR procedures, where the second and/or third standard are double one-ports without transmission.

Calibrating with TMN standards ($k_f = k_r = 0$), for instance, reduces Eqs. (35) to (37) to

$$\mu_f = \frac{\beta_2}{\beta_5}, \quad \mu_r = \frac{\beta_2\beta_3}{\beta_5}, \quad \rho = \pm\sqrt{\mu_f\mu_r - \frac{\beta_4\mu_f}{t} + \frac{1}{t^2}}$$

TAR (TLR), on the other hand, has arbitrary k_f and k_r with $\mu_f = \mu_r = 0$, reducing the set of unknowns to

$$\kappa_r = t\left(\frac{\beta_2}{2} \pm \sqrt{\frac{\beta_2^2}{4} - \beta_1}\right), \quad \kappa_f = \frac{\kappa_r}{\beta_1}$$

$$\rho = \pm\frac{1}{t}\sqrt{1 - \frac{\beta_4(t^2 - \kappa_f\kappa_r)}{\kappa_f(\beta_5 - \kappa_r\beta_4)}}$$

For the TMR procedure (32) $k_f = k_r = 0$ and $\mu_f = \mu_r = 0$. Only the unknown reflection r needs to be determined, yielding

$$\rho = \pm\frac{1}{t}\sqrt{1 - t\frac{\beta_2\beta_4}{\beta_5}}$$

As before, the reflection coefficient must be known a priori to $\pm 90°$ in order to resolve the root ambiguity. Technically this is done by choosing the solution that is closest to the estimated reflection coefficient of the R standard. Its choice as a short or an open is common practice (though not required) and provides the necessary information. Furthermore, the *true* value of r is determined by the self-calibration process and can be used to check the quality of the calibration, in those cases where the R standard is completely known.

It should be noted that the perfect match of the A, L, or M standard in the above-described procedures is the only absolute impedance standard and must always be a known quantity, determining the reference impedance of the calibration. The R standard is not required to be known exactly, and the only demand is that the same reflection is presented to both ports. By connecting the same reflection standard first to port 1 and then to port 2, this requirement is easily met. Possible inconsistencies between the phase-reference planes of the different standards, which may creep in without the use of self-calibration, can therefore not occur. The postulated symmetry of the R standard uniquely sets the phase reference at equal offsets to the test ports. These offsets are zero if the transmission factor t of the through corresponds to its true electrical length.

Besides allowing the calibration of the seven-term error model with partially known standards, self-calibration also provides an interesting means of verifying the quality of the calibration if the calibration standards are fully known. In this case, all deviations of the computed parameters of the standards from their *known* values indicate imperfections of the calibration process.

Employing Self-Calibration for ϵ_r-Measurements

The scheme introduced above for determining the transmission factor of the A standard can be used in a straight-forward manner to obtain error-corrected measurements of the electrical length of an unknown line: Measurements of a through and the unknown line yield the measurement matrices $[P_T]$ and $[\tilde{P}_A]$, which, using Eq. (34) make β_1 and β_2 available. With the transmission factor of a line being

$$e^{-\gamma l} = k_f = k_r = \frac{\kappa_r}{\Delta m_A}$$

Eq. (35) can be used to solve for γl. Furthermore, if the mechanical length l of the line is known, the complex propagation constant γ containing ϵ_r is available with very high precision, even though up to this point no calibration has been performed.

Self-Calibration for the 15-Term Error Model

Contrary to the above-presented self-calibration scheme for the seven-term error model, self-calibration formulas for the 15-term model can be derived without the need for transfer parameters and their associated singularity problems.

As was shown in the section entitled "The Cross-Talk Correcting 15-Term Error Model for Four-Receiver VNAs," the 15-term error model is calibrated using five calibration measurements

$$[G] + [E][M_n] = [S_n]\{[F] + [H][M_n]\} \quad (n = 1, \ldots, 5) \tag{38}$$

Using four of those equations, named i, j, k, and l, most of the error parameters can be eliminated, arriving at

$$\Delta M_{j,k}^{-1}\Delta M_{i,j}\Delta M_{i,l}^{-1}\Delta M_{l,k} = ([H] + [F][M_k])^{-1}\Delta S_{j,k}^{-1}\Delta S_{i,j}\Delta S_{i,l}^{-1}\Delta S_{l,k}([H] + [F][M_k]) \tag{39}$$

with

$$\Delta S_{m,n} = [S_m] - [S_n], \quad \Delta M_{m,n} = [M_m] - [M_n] \quad (m, n = 1, \ldots, 5)$$

(see Ref. 27 for a comprehensive outline of the derivation).

Equation (39) again constitutes a similarity transform, resulting in the two nonlinear relations

$$\begin{aligned} \mathrm{Trace}\{\Delta M_{j,k}^{-1}\Delta M_{i,j}\Delta M_{i,l}^{-1}\Delta M_{l,k}\} &= b_1 = \mathrm{Trace}\{\Delta S_{j,k}^{-1}\Delta S_{i,j}\Delta S_{i,l}^{-1}\Delta S_{l,k}\} \\ \mathrm{Det}\{\Delta M_{j,k}^{-1}\Delta M_{i,j}\Delta M_{i,l}^{-1}\Delta M_{l,k}\} &= b_2 = \mathrm{Det}\{\Delta S_{j,k}^{-1}\Delta S_{i,j}\Delta S_{i,l}^{-1}\Delta S_{l,k}\} \end{aligned} \tag{40}$$

between the measured values $[M_n]$ and the standards' S-parameters (invariance of the eigenvalues of similar matrices).

Because only four calibration measurements are used by Eq. (39), the fifth standard $[S_m]$, $[M_m]$ may be substituted into Eq. (39) to yield two more similarity transformations:

$$\Delta M_{j,k}^{-1}\Delta M_{m,j}\Delta M_{m,l}^{-1}\Delta M_{l,k} = ([H] + [F][M_k])^{-1}\Delta S_{j,k}^{-1}\Delta S_{m,j}\Delta S_{m,l}^{-1}\Delta S_{l,k}([H] + [F][M_k]) \tag{41}$$

(ith standard replaced by mth standard) and

$$\Delta M_{m,k}^{-1}\Delta M_{i,m}\Delta M_{i,l}^{-1}\Delta M_{l,k} = ([H] + [F][M_k])^{-1}\Delta S_{m,k}^{-1}\Delta S_{i,m}\Delta S_{i,l}^{-1}\Delta S_{l,k}([H] + [F][M_k]) \tag{42}$$

(jth standard replaced by mth standard).

Together with Eq. (40), the resulting trace and determinant equalities provide six nonlinear self-calibration equations, sufficient for computation of the maximally five unknowns that the 15-term error model allows for.

It is interesting to note that the derivation of Eq. (39) holds as long as the structure of the error model [Eq. (38)] is unchanged. The calibration standards and/or the measurement matrix $[M]$ may therefore also be expressed in T-(transfer) parameters or even in chain parameters, using voltages and currents instead of waves. Even the extension to the error model of an N-port VNA, as described in Ref. 24, is straightforward. In this case, all quadrants of the error matrix, the standards' S- (T-) matrix, and the measurement matrices are $N \times N$ matrices. The invariance of the eigenvalues of the two similar matrices in Eq. (39) yields N relations between the measured values and the standards.

The Tmrg Procedure. The self-calibration equations [Eqs. (39), (41), and (42)] permit construction of a multitude of self-calibration procedures, allowing calibration with the set of standards, best suited for a specific application. A particularly interesting variant, the Tmrg procedure, refining the Tmso procedure of the section entitled "The Cross-Talk Correcting 15-Term Error Model for Four-Receiver VNAs," shall now be introduced.

Whereas Tmso requires a *perfect* match, short and open, the above-derived formalism allows the reflection coefficients of the short and open to be computed through self-calibration. Furthermore, a nonzero but known reflection coefficient may be used as the m standard, reducing its requirement from *perfect* to *known*.

Comparable with Fig. 22, Fig. 25 shows the five standards to be constructed from a Through (with known transmission factor t) and three reflection one-ports with reflection coefficients m, r, and g. The first four standards suffice for the determination of the unknown reflection coefficients r and g:

Substituting the standards i, j, k, and l into Eq. (39) and evaluating the product of S-matrix differences yield

$$\Delta S_{j,k}^{-1}\Delta S_{i,j}\Delta S_{i,l}^{-1}\Delta S_{l,k} = [B] = \frac{1}{t^2 - rm}\begin{bmatrix} t^2C_1 - m^2C_2 & t(mC_2 - gC_1) \\ t(rC_1 - mC_2) & t^2C_2 - rgC_1 \end{bmatrix}$$

with

$$C_1 = \frac{r - m}{r - g}, \quad C_2 = \frac{g - r}{g - m}$$

resulting in

$$\mathrm{trace}\{\Delta M_{j,k}^{-1}\Delta M_{i,j}\Delta M_{i,l}^{-1}\Delta M_{l,k}\} = \mathrm{trace}[B] = b_1 = \frac{m^2(g - m) + gr(m - r) + t^2(r - g)}{(rm - t^2)(m - g)} \tag{43}$$

$$\det\{\Delta M_{j,k}^{-1}\Delta M_{i,j}\Delta M_{i,l}^{-1}\Delta M_{l,k}\} = \det[B] = b_2 = \frac{(t^2 - mg)(r - m)}{(t^2 - rm)(m - g)} \tag{44}$$

Equation (44) can be solved to yield a linear relation for r

$$r = \frac{b_2t^2(g - m) + m(gm - t^2)}{b_2m(g - m) + (gm - t^2)} \tag{45}$$

and can be combined with Eq. (43) to form a quadratic equation for g

$$g^2 - g\frac{2mt^2a_1a_2}{m^2a_3 - t^2b_2^2} + \frac{t^4a_3 - t^2m^2b_2^2}{m^2a_3 - t^2b_2^2} = 0 \tag{46}$$

with

$$a_1 = b_1 - 1 - 2b_2, \quad a_2 = b_2 + 1$$
$$a_3 = (b_1 - 1)(b_2 + 1) - b_2(2 + b_2)$$

Figure 25. Calibration standards for the 15-term Tmrg self-calibration procedure. $[S^{T}_{(k)}] = \begin{bmatrix} 0 & t \\ t & 0 \end{bmatrix}$, $[S^{rm}_{(j)}] = \begin{bmatrix} r & 0 \\ 0 & m \end{bmatrix}$, $[S^{mg}_{(l)}] = \begin{bmatrix} m & 0 \\ 0 & g \end{bmatrix}$, $[S^{gr}_{(i)}] = \begin{bmatrix} g & 0 \\ 0 & r \end{bmatrix}$, $[S^{rg}_{(m)}] = \begin{bmatrix} r & 0 \\ 0 & g \end{bmatrix}$

Choosing the proper root for g requires knowledge about the sign of that reflection standard. Using a short for g and an open for r provides the necessary sign information and makes the standards sufficiently distinct for subsequent use as fully known calibration standards.

The only parameters that must be known are the transmission coefficient t of the T standard and the reflection m. The quantity m should be small for numerical reasons and must be known, but the standard is not required to be an *ideal* match.

Since only one set of reflection one-ports is physically required, the postulated equality of the reflection coefficients that enter the different standards is guaranteed, an important advantage over calibration procedures, which require the *same* reflection coefficient to be connected to both ports simultaneously.

OUTLOOK AND RELATED TOPICS

The continously growing need for fast (production) and precision (laboratory) network measurements has led to the development of sophisticated instrumentation equipment (33–35) and many optimized calibration procedures. This process is expected to continue with the focus shifting toward even higher frequencies (>110 GHz), on-wafer cross-talk correction, and N-port measurements (36,37). A lot of interest is spawned by the communication industry—for instance, in the characterization of IC packages (N-port measurements) and in high production throughput. Semiautomatic calibration procedures, avoiding the necessity of reconnecting the calibration standards for every calibration, address this need but are not covered here. The interested reader is referred to Ref. 38 for an overview. References 39 and 40 describe commercially available solutions.

Finally, Refs. 20 and 41 present statistical methods to assess errors not originally contained in the error model, like repeatibility or contacting errors. Because these errors meanwhile constitute the accuracy limit of error-corrected network analyzer measurements, their inclusion is expected to further boost measurement accuracy.

BIBLIOGRAPHY

1. M. Sucher and J. Fox, *Handbook of Microwave Measurements,* Vol. 1, Brooklyn, NY: Polytechnic Press of the Polytechnic Institute of Brooklyn, 1963.
2. P. I. Somlo and J. D. Hunter, *Microwave Impedance Measurements, IEE electrical measurement series,* Vol. 2, Stevenage, UK: Peregrinus, 1985.
3. G. U. Sorger, Coaxial swept-frequency VSWR measurements using slotted lines, *IEEE Trans. Instrum. Meas.,* **IM-17**: 403–412, 1968.
4. R. Caldecott, The generalized multiprobe reflectometer and its application to automated transmission line measurements, *IEEE Trans. Antennas Propag.,* **AP-21**: 550–554, 1973.
5. C. L. J. Hu, A novel approach to the design of multiple-probe high-power microwave automatic impedance measuring schemes, *IEEE Trans. Microw. Theory Tech.,* **MTT-28**: 1422–1428, 1980.
6. C. A. Hoer, The six-port coupler: a new approach to measuring voltage, current, power, impedance and phase, *IEEE Trans. Instrum. Meas.,* **IM-21**: 466–470, 1972.
7. G. F. Engen, The six-port reflectometer: an alternative network analyzer, *IEEE Trans. Instrum. Meas.,* **IM-21**: 1075–1080, 1972.
8. P. I. Somlo and J. D. Hunter, A six-port reflectometer and its complete characterization by convenient calibration procedures, *IEEE Trans. Microw. Theory Tech.,* **MTT-30**: 186–192, 1982.
9. G. F. Engen, An improved circuit for implementing the six-port technique of microwave measurements, *IEEE Trans. Microw. Theory Tech.,* **MTT-25**: 110–112, 1977.
10. D. M. Pozar, *Microwave Engineering,* Reading, MA: Addison-Wesley, 1990.
11. S. Uysal, *Nonuniform Line Microstrip Directional Couplers and Filters,* Norwood, MA: Artech House, 1993.
12. H. M. Churchill and L. Susman, A six-port automatic network analyzer, *IEEE Trans. Microw. Theory Tech.,* **MTT-25**: 1086–1091, 1977.
13. G. F. Engen and C. A. Hoer, Thru-reflect-line: An improved technique for calibrating the dual six port automatic network analyzer, *IEEE Trans. Microw. Theory Tech.,* **MTT-27**: 987–993, 1979.
14. H.-G. Krekels and B. Schiek, A full model calibration algorithm for a dual six-port network analyzer, *Proc. IEEE Instrum. Meas. Conf. (IMTC),* Hamamatsu, Japan, 1994, pp. 990–993.
15. R. J. King, *Microwave Homodyne Systems,* Stevenage, UK: Peregrinus, 1978.
16. U. Gärtner and B. Schiek, A broad-band homodyne network-analyzer with binary phase-modulation, *IEEE Trans. Microw. Theory Tech.,* **MTT-34**: 902–906, 1986.
17. D. Rytting, An analysis of vector measurement accuracy enhancement techniques, Hewlett Packard, April 1981.
18. D. Rytting, Appendix to an analysis of vector measurement accuracy enhancement techniques, Hewlett Packard, April 1981.
19. W. H. Press, et al., *Numerical Recipes in C,* Cambridge, UK: Cambridge Univ. Press, 1988.
20. H. Van Hamme and M. Vanden Bosche, Flexible vector network analyzer calibration with accuracy bounds using an 8-term or a 16-term error correction model, *IEEE Trans. Microw. Theory Tech.,* **MTT-42**: 976–987, 1994.
21. H.-J. Eul and B. Schiek, A generalized theory and new calibration procedures for network analyzer self-calibration, *IEEE Trans. Microw. Theory Tech.,* **MTT-39**: 724–731, 1991.
22. A. Ferrero, Two-port network analyzer calibration using an unknown "Thru", *IEEE Microwave Guided Wave Lett.,* **2**: 505–507, 1992.
23. B. Saswata and L. Hayden, An SOLR calibration for accurate measurement of orthogonal on-wafer DUTs, *Proc. IEEE MTT-S Int. Microw. Symp.,* Denver, CO, 1997, pp. 1335–1338.
24. R. A. Speciale, A generalization of the TSD network-analyzer calibration procedure, covering n-port scattering-parameter measurements, affected by leakage errors, *IEEE Trans. Microw. Theory Tech.,* **MTT-25**: 1100–1115, 1977.
25. K. J. Silvonen, Calibration of 16-term error-model, *Electron. Lett.,* **29**: 1544–1545, 1993.
26. H. Heuermann and B. Schiek, Results of network analyzer measurements with leakage errors corrected with the TMS-15-term procedure, *Proc. IEEE MTT-S Int. Microw. Symp.,* San Diego, CA, 1994, pp. 1361–1364.

27. A. Gronefeld and B. Schiek, Network-analyzer self-calibration with four or five standards for the 15-term error-model, *Proc. IEEE MTT-S Int. Microw. Symp.,* Denver, CO, 1997, pp. 1655–1658.
28. G. L. Madonna, A. Ferrero, and U. Piani, Multiport network-analyzer self-calibration: A new approach and some interesting results, *49th ARFTG Conf. Dig.,* Denver, CO, 1997, p. 142.
29. K. J. Silvonen, LMR 16—a self-calibration procedure for a leaky network analyzer, *IEEE Trans. Microw. Theory Tech.,* **MTT-45**: 1041–1049, 1997.
30. A. Gronefeld and B. Schiek, Eine neue Methode zur Generierung von Selbstkalibrierverfahren für Netzwerkanalysatoren, anwendbar auf alle bekannten Fehlermodelle, *Kleinheubacher Berichte 1998,* Band 41, pp. 117–126.
31. H. Heuermann and B. Schiek, Robust algorithms for Txx network analyzer self-calibration procedures, *IEEE Trans. Instrum. Meas.,* **IM-43**: 18–23, 1994.
32. H. J. Eul and B. Schiek, Thru-match-reflect: One result of a rigorous theory for de-embedding and network analyzer calibration, *Proc. 18th Eur. Microw. Conf.,* Stockholm, 1988, pp. 909–914.
33. O. Ostwald and C. Evers, Vector network analyzer family ZVR,to the heart of the chart, *News from Rohde & Schwarz,* **150**: 6–9, 1996.
34. A. Wiltron, 360/37XXXA/B Series Vector Network Analyzers, Application Note AN360B/37XXXA/B-1, Mai 1996.
35. Hewlett Packard, "HP8510", Product information.
36. A. Ferrero, F. Sanpietro, and U. Pisani, Multiport vector network analyzer calibration: A general formulation, *IEEE Trans. Microw. Theory Tech.,* **MTT-42**: 2455–2461, 1994.
37. J. C. Tippet and R. A. Speciale, A rigorous technique for measuring the scattering matrix of a multiport device with a 2-Port network-analyzer, *IEEE Trans. Microw. Theory Tech.,* **MTT-30**: 661–666, 1982.
38. H.-G. Krekels and B. Schiek, A novel procedure for an automatic network-analyzer calibration, *IEEE Trans. Instrum. Meas.,* **IM-44**: 291–294, 1995.
39. H. G. Krekels, AutoKal: Automatic calibration of vector network analyzer ZVR, *Rohde & Schwarz Application Note 1EZ30 IE,* 1996.
40. Hewlett Packard, *E*cal, *Product Information.*
41. R. B. Marks, A multiline method of network analyzer calibration, *IEEE Trans. Microw. Theory Tech.,* **MTT-39**: 1205–1215, 1991.

BURKHARD SCHIEK
ANDREAS GRONEFELD
Ruhr-Universität Bochum

STARTUP CIRCUITS. See BOOTSTRAP CIRCUITS.
STATE ESTIMATION. See KALMAN FILTERS.
STATE ESTIMATION OF POWER SYSTEMS. See POWER SYSTEM STATE ESTIMATION.
STATE SPACE METHODS. See DELAY SYSTEMS.
STATES, SURFACE. See SURFACE STATES.
STATIC ELECTRICITY. See ELECTROSTATIC PROCESSES; TRIBOELECTRICITY.